THE EFFECT OF TREATMENT ON MYOFASCIAL TRIGGER POINTS IN UPPER TRAPEZIUS MUSCLE: EMG FATIGUE PARAMETERS, JOINT RANGE OF MOTION, PAIN AND PERCEPTION OF DISABILITY

by

Zahra M. Kazem Moussavi

A THESIS

SUBMITTED TO THE FACULTY OF GRADUATE STUDIES IN PARTIAL FULFILLMENT OF THE REQUIREMENT FOR THE DEGREE OF DOCTOR OF PHILOSOPHY

DEPARTMENT OF ELECTRICAL ENGINEERING

UNIVERSITY OF MANITOBA

WINNIPEG, MANITOBA

JUNE, 1997

THE UNIVERSITY OF MANITOBA

FACULTY OF GRADUATE STUDIES

*****

COPYRIGHT PERMISSION PAGE

THE EFFECT OF TREATMENT ON MYOFASCIAL TRIGGER POINTS IN UPPER TRAPEZIUS MUSCLE: EMG FATIGUE PARAMETERS, JOINT RANGE OF MOTION, PAIN AND PERCEPTION OF DISABILITY

BY

ZAHRA M. KAZEM MOUSSAVI

A Thesis/Practicum submitted to the Faculty of Graduate Studies of The University of Manitoba in partial fulfillment of the requirements of the degree of

DOCTOR OF PHILOSOPHY

بسم الله تعالى

ABSTRACT

Myofascial trigger points (TP), are muscle manifestations of a regional pain disorder and are very common, particularly in trapezius. In severe cases myofascial TPs can cause disability; however, early recognition and treatment may prevent progression to chronic pain. This study investigated the effect of treatment on myofascial TPs using objective measurements such as EMG fatigue parameters (fatigue rate, RMS and mean power frequency (MPF) behavior and endurance time), head-neck range of motion, and subjective measurements such as pain levels of patients and perceived disability. In order to measure the head-neck range of motion, a new method was developed to measure this motion simultaneously in three planes. Subjects were nine patients with myofascial TPs in upper trapezius and nine healthy individuals. Patients were tested once before treatment and at three intervals after the first treatment; the last test session occurred after treatment was completed. Healthy subjects were tested three times with a three week interval between the sessions. EMG signals were recorded simultaneously by surface electrodes from the upper trapezius and middle deltoid muscles in two different test positions until the limit of subjective fatigue. EMG results showed significant improvement after treatment; however the treated afflicted muscle still had a different fatigue pattern compared to that of normal muscles. Results also showed significant improvements in head-neck range of motion and subjective measurements in patients after treatment. Based on the EMG results from the healthy subjects, this study presents a functionally-related EMG fatigue pattern for trapezius and challenges the common interpretation of the RMS behavior with fatigue.

ACKNOWLEDGMENT

I wish to express my sincere gratitude to my advisors, Dr. Ed Shwedyk and Dr. Archie Cooper for their constructive suggestions and kind guidance throughout this research. They were always a constant source of encouragement and enthusiasm for me.

I would also like to thank Dr. Dubo for his guidance. I am grateful for the time he gave me to learn and observe myofascial pain syndrome treatment.

I wish to thank all the subjects who participated in this research. Without their kind cooperation, this study could not have been done.

I would also like to thank Mr. John Vukelic for the muscle illustrations.

Lastly, I would like to thank my husband and children for their patience, support and encouragement during the entire work of this thesis.

CONTENTS

LIST OF TABLES

LIST OF FIGURES

CHAPTER 1

INTRODUCTION

1.1 Introduction

This thesis deals with the effect of treatment on myofascial trigger points. The two main objectives of this thesis are to study the relationship between electromyography (EMG) and trigger points (TPs) associated with myofascial pain syndrome (MPS), and to develop an objective and reliable method to measure head-neck motion, as restriction in this motion is usually associated with myofascial TPs.

Myofascial pain syndrome is defined as a regional pain disorder in the presence of the following characteristics in an involved muscle: **1)** trigger points on palpation with referred pain; **2)** reproduction of the patient's pain symptoms on palpation of the trigger point; **3)** a taut band of muscle which harbors the trigger point; and **4)** twitch response on palpation of, or needle insertion into the taut band [Simons, 1987]. Many hypotheses about the etiology of MPS have been presented. Although the manifestations of the syndrome are well known, knowledge regarding the etiology of the syndrome is limited.

Myofascial trigger points (TPs) can occur in all skeletal muscles of the body, but they are most frequently seen in the head, neck, shoulder, and lower back regions [Fricton et al, 1985]. According to Travell and Simons [1983] the trapezius is probably the muscle most often afflicted by myofascial TPs.

Trigger points associated with myofascial pain syndrome are extremely common. The severity of symptoms from trigger points ranges from painless restriction of motion due to latent trigger points, to agonizing, incapacitating pain caused by very active trigger points. Such severe pain can disrupt normal activities, and should it become chronic, may result in disability [Travell & Simons, 1983].

Disability is one of industry's and society's most expensive burdens. Bonica [1974] pointed out that disabling chronic pain costs the American people billions of dollars annually. In 1982, 82,000 of the 1.5 million claimants for Social Security Disability suffered from what was defined as "chronic pain syndrome" [Fricton & Awad, 1990]. These figures do not reveal the emotional cost of the pain to the patient and to his/her immediate family, nor the cost resulting from disability and unemployment. These high costs call for improved techniques to quantify chronic pain stages and to match them with ratings of impairment and disability [Brena et al, 1979].

Quantifying the disability associated with myofascial pain syndrome is difficult at best considering that no objective or standardized laboratory test or physical examination finding exists that singularly measures the totality of the pain experience. Additionally, there are few ways of measuring improvement as a result of treatment; most methods rely on subjective reports. Should litigation be sought, this lack of objective findings creates difficulty for both claimants and insurers. One of the objectives of this investigation is to develop an objective tool to measure the range of motion in head and neck. With such a tool, the impairment caused by MPS can be quantified and related to disability. As well, the effect of treatment (if any) on range of motion can be measured.

A relationship has also been found between myofascial pain syndrome and the EMG fatigue characteristics of the involved muscles [Oberg et al, 1992]. As they have reported, the mean power frequency (MPF) and the root mean square (RMS) of the recorded EMG signals were more pronounced in normal muscles compared to those in myalgic muscles [Oberg et al, 1992]. It is well established that fatigue in normal muscles is accompanied by a shift of EMG power spectrum toward lower frequencies [Basmajian & De Luca, 1985]. Because the EMG signal changes with muscle fatigue and because a difference in fatigue parameters may be found between affected and unaffected sides of the same muscle, EMG has the potential to be used as an objective tool to measure improvement in MPS if, in fact, specific patterns of muscle fatigue are found to be characteristic of MPS. While finding such characteristics of MPS in relation to fatigue pattern of the affected muscle is of clinical interest, studying the fatigue pattern of a muscle, such as trapezius, is also of academic interest and has been associated with many ambiguities and controversies.

1.2 Objectives

The objectives of this thesis are:

- to study EMG fatigue characteristics of trapezius muscle in healthy individuals and compare them with those in subjects with TPs in upper trapezius;
- to study the effect of treatment on EMG fatigue parameters in patients;
- to develop a new three-dimensional (3-D) method to measure head-neck motion;

general it may be explained as follows. It is believed that in the presence of the troponin-tropomyosin complex, the normal actin filament of the relaxed muscle is inhibited from binding to the myosin filament. The theory of muscle contraction that is widely accepted today has to do with the configuration change in the actin molecule due to the binding of calcium ions to troponin. The binding of calcium ions to the troponin complex changes the normal relationship between the troponin and actin, and produces a new condition that leads to contraction. Such a condition causes the actin and the myosin filaments to bind to each other (Figure 2.1). Once the binding sites on actin have been made available, the crossbridge of myosin rapidly attaches to actin. It is usually hypothesized that, after the crossbridges formed, the stored adenosine triphosphate (ATP) in one of the heads of myosin, provides energy for the cross bridge to rotate forward while it is still attached to actin. Therefore these filaments slide along each other and cause shortening of the muscle. Although the exact mechanism by which the muscle shortening happens is not yet clear, it is believed that this is the mechanism by which the action potential causes muscle contraction [Enoka, 1988]. However, the calcium ions do not remain in the region of the myofibrils for more than a few milliseconds, because once the electrical current caused by the action potential is over, the sarcoplasmic reticulum almost immediately sequesters the calcium ions out of the sarcoplasm. Therefore, in effect, the action potential causes a short pulse of calcium ions in the region of the myofibril, and it is during this time that the contractile process is activated. At the termination of this pulse of calcium ions, the muscle immediately relaxes.

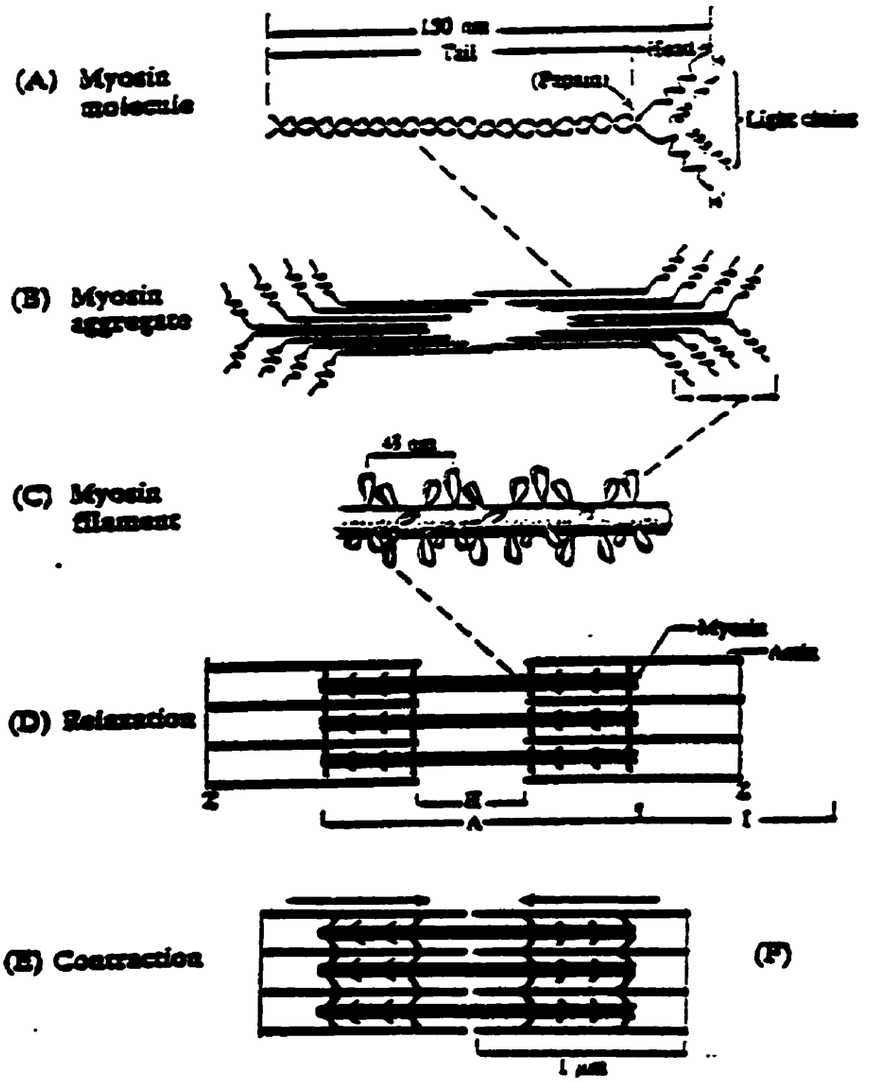

Figure 2.1 The myosin molecule and its arrangement in the thick filaments of the myofibrils. (A) A single molecule, consisting of a double-helical rod terminating in two globular heads, each of which has two light chains attached. (B) In solution, myosin molecules spontaneously aggregate to form filaments with heads at both ends. (C) In a thick filament, the two globular heads of a myosin molecule project to form a cross-bridge. The next bridge is separated by 14.3 nm and 60o. (D) The overlap of actin and myosin filaments in a relaxed myofibril and the various refractive bands that are created. (E) Contraction is produced by actin filaments sliding over the myosin filament, causing approximation of the Z-lines and narrowing of the H-region. *(from Skeletal Muscles [McComas, 1996])*

The electrical voltage which is detectable on the surface of muscles during a contraction can be explained by the fairly well established theory of motor units. The axon of each motoneuron that leaves the spinal cord usually innervates many muscle fibers. All the muscle fibers innervated by a single motoneuron along with its large axon and its terminal branches, are called a *motor unit* [Basmajian & De Luca, 1985] (Figure 2.2). In general, muscles that react rapidly and whose control is precise, have few muscle fibers (as few as 10 to 15) in each motor unit and have a large number of motoneurons directed to the muscle. On the other hand, slow acting muscles, which do not require a very fine degree of control may have as many as 300 to 800 muscle fibers in each motor unit [Guyton, 1971]. Usually muscle fibers of adjacent motor units overlap, with small bundles of 10 to 15 fibers from one motor unit lying among similar bundles of the second motor unit. This configuration allows the separate motor units to contract in support of each other rather than entirely as an individual segment [Guyton, 1971]. The force of contraction increases progressively as the number of contracting motor units increases. That is, as more and more motor units are activated simultaneously, the strength of contraction increases. In addition, successive muscle twitches overlap in time, which means that the first muscle twitch is not completely over by the time that the second one begins. Therefore, since the muscle is already in a partially contracted state when the second twitch begins, the degree of muscle shortening this time is slightly greater than that which occurs with a single muscle twitch. Consequently, at more rapid rates of contraction, the degree of summation of successive contractions becomes greater and greater until an optimum frequency is reached [Guyton, 1971].

Motor units differ from each other not only in size, but also in their recruitment order and firing rate. The most consistent observation of motor unit behavior reported in the literature concerns the order of recruitment as a function of motoneuron size. In a steady contraction, small motor units are recruited before the large ones [McComas, 1996]. It has been shown that the slower conduction velocities, and thus the smaller axons, are associated with the lower threshold motor units [Freund et al, 1973]. The order of motor unit recruitment is also a function of fiber type and size of muscle. Type I fibers, which are known as slow twitch fibers are recruited first followed by type II (fast twitch) fibers. In sudden movements type II fibers may have the lowest threshold and be recruited first [McComas, 1996]. Small muscles recruit all their motor units below 50% maximum voluntary contraction (MVC) and larger muscles recruit motor units throughout the full range of voluntary force [Basmajian & De Luca, 1985]. However, the order of motor unit recruitment may change if the functional role of the same muscle changes, e.g. McComas [1996] cited Gielen and Denier Van Der Gon [1990] to state that "in the biceps the threshold of a motor unit depends on whether the muscle is being used to flex the elbow, supinate the forearm, or externally rotate humerus." [McComas, 1996, page 208]

Firing rates of motor units are also muscle dependent. In general the smaller the muscle, the higher the firing rate. During sustained contractions, the firing rate of motor units decreases as a function of time and this phenomenon is more evident in fast-twitch fibers than in slow-twitch fibers [Basmajian & De Luca, 1985]. Table 2.1 summarizes the discussed muscle fiber characteristics.

Force can be generated by increasing the firing rate of the motor units as well as by recruitment of new motor units. It is a common belief that at the beginning of a contraction, recruitment of new motor units is the dominant factor with the smallest motor units being recruited first while the increase of firing rate plays a secondary role. However, for force levels ranging from 30% to 75% of MVC, the dominant factor is an increase in firing rate. Some recruitment of larger motor units also occurs but this factor plays a secondary role [Basmajian & De Luca, 1985].

Characteristic	Type I	Type II
Diameter	Small	Large
Muscle Color	Red	White
Speed of Contraction	Slow	Fast
Rate of Fatigue	Slow	Fast
Motor Unit Size	Small	Large
Axon Conduction Velocity	Slow	Fast
Major Function	Tonic	Phasic

Table 2.1 Summary of the muscle fiber characteristics (*from Norkin & Levangie, 1992*).

2.2 Muscle Fatigue

Sustained and strong contraction of a muscle leads to the well-known state of muscle fatigue. This is simply the inability of the contractile processes of the muscle fiber to continue to produce the same amount of work. In fact, the nerve continues to function properly, the nerve impulses pass normally through the neuromuscular junction onto the muscle fiber, and even normal action potentials spread over the muscle fibers, but the contraction becomes weaker and weaker because of depletion of energy supplies in the muscle fibers themselves. If a muscle becomes fatigued to an extreme extent, it is likely to become continually contracted, remaining contracted and rigid for many minutes even without an action potential as a stimulus. This is called *physiological contracture* of the muscle [Guyton, 1971]. At the physiological fatigue stage, a burst of activity can still be achieved as a result of encouragement or fear, its duration is however, highly variable and depends on the emotional state of the individual.

An assumed mechanism for peripheral fatigue is as follows. The ATP is required to make the actin and myosin molecules separate during the process of muscle relaxation, otherwise the myosin and actin filaments will continue to be bound to each other. In extreme degrees of muscle fatigue, essentially all the ATP is depleted; this accounts for the rigid binding of the actin and myosin filaments in the contracted state of the muscle. The reasons for ATP depletion are many. A full discussion is beyond the scope of this study.

2.3 Myofascial Pain Syndrome (MPS) Due to Trigger Points (TPs)

Myofascial pain caused by trigger points is a neuromuscular dysfunction. A myofascial trigger point (TP) is clinically identified as a tender spot within a taut band of skeletal muscle, located in the muscular tissue and/or its associated fascia. Two distinct kinds of pain are associated with TPs: direct and referred. Direct pain is experienced when digital pressure is applied to the area over the TP; a sharp local pain is also experienced by needle injection to the TP. On the other hand, a TP can refer pain to regions beyond the immediate vicinity of the trigger point [Simons, 1993].

Myofascial TPs are categorized into two groups: *active TPs* and *latent TPs*. Active TPs are painful either at rest or during motion, and are always tender. Active TPs, when compressed by insertion of a needle or by firm palpation, cause a local twitch response (LTR) and acute pain, while latent TPs may become active with this procedure. The LTR is considered to be a valuable objective clinical identifier of myofascial TPs because it is a unique characteristic of myofascial TPs and is demonstrable by EMG recording [Simons, 1987]. A latent TP may show all the diagnostic features of an active TP except for the continuous pain. A frequent repetitive contraction without adequate intervening rest periods may convert a latent TP to an active TP. Trigger points are distinguished from tender points, associated with fibromyalgia, based on whether the patient noted pain referral to a remote area during direct deep palpation of the tender muscle [Simons, 1987].

2.3.1 Symptoms

MPS due to TPs has several clinical characteristics which are strongly muscle oriented, such as trigger points within a palpable taut band with referred pain, LTR, weakness without atrophy, and increased fatiguability of affected muscles [Simons, 1987]. According to Travell and Simons [1983], the most important clinical symptoms may be summarized as the following:

- The pattern of referred pain is specific for each muscle.
- Trigger points are activated by direct trauma and/or overload of the muscle.
- The stretch range of motion is restricted. Usually the muscle cannot be extended to its full range.
- The maximum contractile force of an affected muscle is decreased.
- Muscles in the immediate vicinity of a TP are also felt to be tense upon palpation.
- Snapping palpation of a TP can evoke the local twitch response.
- Moderate but sustained pressure on a TP can aggravate pain in the referral zone.

2.3.2 Etiology

Although the symptoms of MPS are well known, there are still many different hypotheses regarding the etiology of the syndrome, to be proved or disproved by researchers. According to Simons [1987], muscle contraction is not directly responsible for the pain of TPs but rather it sensitizes the nerve endings of group III and group IV muscle nociceptors. Sensitization causes the nerve to respond to a reduced threshold by

increasing its response to a given stimulus. Thus, sensitization may induce spontaneous firing in a nerve that was not spontaneously active [Simons, 1987]. This mechanism explains the tenderness and pain associated with tissue injury and inflammatory processes.

As mentioned before, myofascial pain is not always felt in the vicinity of an active TP but may be some distance away, in the so called "referral zone". According to Simons [1987], motoneurons supplying muscles in the referral zone show increased excitability during voluntary contraction, which can be considered to be a form of spasm. In addition, other muscles, whose functions are synergistic to that of the affected muscle, are likely to exhibit spasm that is also measurable as EMG activity.

It is well accepted that shortening of sarcomeres is responsible for forming a taut band in the region of a TP. As was mentioned in Section 2.1, contraction of skeletal muscle depends on forceful interaction between actin and myosin filaments. The contraction process is normally activated by calcium ions that are released from the sarcoplastic reticulum in response to an action potential and, as long as the calcium is not returned to the sarcoplastic reticulum, the contractile activity continues. The uptake of calcium ions into the sarcoplastic reticulum is dependent upon high energy ATP. If the sarcoplasmic reticulum is ruptured due to muscle overload, it follows that the calcium releases with no immediate mechanism to pump the ions back into the sarcoplasmic reticulum. The sarcomeres will therefore remain in the contracted state. Such localized severe shortening in a group of muscle fibers causes capillaries supplying the muscle to be occluded, leading a severe localized ischemia. The local ischemia prevents restoration of ATP to the sarcoplasmic reticulum, and the muscle fibers continue to be contracted.

Therefore, there would be an energy crisis in the sarcoplasmic reticulum, as its ATP-dependent calcium pump would still be unable to recover ionized calcium even after the reticulum's rupture repaired itself [Simons, 1987].

Sarcomeric shortening also explains why sustained voluntary contraction, especially in the shortened position, or too frequent repetitive contraction without adequate intervening rest periods (as in assembly line work) may convert a latent TP to an active TP. The energy crisis also explains the more rapid onset of fatigue in muscles afflicted with active TPs compared with muscles without active TPs.

2.3.3 Importance

Skeletal muscle is the largest organ of the human body and skeletal muscle tissues are subject to the wear and tear of daily activities [McComas, 1996]. Yet muscle dysfunction has received little attention compared to other disease. Myofascial TPs are extremely common and become a distressing part of every day life [Travel & Simons, 1983]. Although myofascial trigger points are not life threatening, their painfulness can severely affect one's life. Patients with other kinds of severe pain experiences, such as pain due to heart attack or a broken bone, find the myofascial pain from TPs just as severe [Travell & Simons, 1983]. Therefore, in severe cases, MPS can result in disability. According to Travell and Simons [1983] most of the disabilities due to chronic pain in shoulder, neck, and back are commonly as a result of unrecognized myofascial TPs. However, early recognition and treatment of myofascial TPs can prevent the development of chronic pain.

While it is relatively simple to treat a single-muscle with MPS, the complex chronic MPS caused by severe perpetuating factors is very difficult to resolve. Resolving a chronic MPS needs several treatments and lasting success in treatment depends on education of the patient [Simons, 1987]. The myofascial TP treatment includes stretch and spray, postisometric relaxation, needle injection, specific kinds of massage and ultrasound or electrical stimulation applied to the TP. Other than subjective measurements, to date there has not been an objective method to evaluate the effect of treatment on myofascial trigger points. Therefore, one of the objectives of this thesis is to investigate the effect of treatment on EMG fatigue parameters of the myalgic muscle as well as to measure the range of motion of the affected area.

2.4 Trapezius Muscle

Trapezius is probably the most common muscle affected by myofascial TPs due to high work demand or acute trauma [Travell & Simons, 1983]. Since one of the objectives of this thesis is to study the EMG fatigue characteristics of trapezius, a reasonable understanding of the muscle characteristics is needed.

Structure- Trapezius is a flat and triangular muscle that covers the posterior part of the neck, shoulder, and thorax. Basically as the direction of the fibers suggests, one can divide the trapezius into three parts: the upper or descending portion, the middle or transverse portion and the lower or ascending portion. Variation in the structure of the trapezius muscle can occur and it is often found to be asymmetrical between the both sides [Gray's Anatomy, 1985].

Innervation- The exact motor innervation of the trapezius has been controversial. Based on cadaveric anatomy, the trapezius is innervated by the accessory or 11th cranial nerve, but in addition, some direct branches reach it from the cervical plexus [Basmajian, 1970]. Electromyography and nerve stimulation have been used to study the motor innervation of the trapezius [Hamlyn et al, 1986; Soo et al, 1990; Krause, 1992; Stacey et al, 1995]. It is commonly reported that the accessory nerve is the most important motor supply of trapezius. The contribution of the cervical plexus has been shown to be variable among patients and the motor input from C3-C4 branches needs further study.

Fiber Type Composition- It is commonly held that muscles with an almost exclusively postural function (tonic muscles) are predominantly composed of type-I fibers, whereas muscles involved with mainly rapid and purposeful activities (phasic muscles) have a high type-II fiber content [Polgar et al, 1973]. According to the results reported by Johnson et al. [1973], trapezius consists mainly of type I fibers. However, the results of Lindman et al [1990], showed differences in fiber type composition between the different portions of the trapezius muscle. In general the lower third of the descending, the transverse and the ascending portions were found to have a predominance of type-I muscle fibers, whereas the results from the most superior parts of the descending portion indicated a higher proportion of type-II fibers. Such differences in muscle fiber composition could be due to different functional requirements of the muscle and/or, as Lindman et al [1990] suggested, to genetic factors. A number of researchers also studied the muscle morphology in chronic trapezius myalgia [Larsson et al, 1988; Lindman et al, 1990; Uhlig et al, 1995]. The

reports indicated that changes in muscle morphology in chronic trapezius myalgia do exist but the exact pattern of the change is yet to be determined.

Function- The distribution of the fiber types and the anatomical arrangement of the trapezius muscle suggest a functional differentiation of the muscle. It is generally believed that the upper trapezius shrugs the shoulder; normally it maintains the shoulder level but in fatigue it allows the shoulders to droop. The middle fibers retract the scapula and steady the scapula at the very beginning of the movement of raising the arm above the head. The lower fibers pull the medial end of the spine of the scapula downwards, i.e., they cooperate with the upper fibers to rotate the glenoid cavity upwards- a necessary position in raising the arm above the head [Basmajian, 1970]. Electromyography has been used by several researchers to study the functional role of trapezius during shoulder motion [Inman et al, 1944; Fisk & Colwell, 1954; Bearn, 1961; Bagg & Forrest, 1986]. In light of the work of Inman and his co-workers [1944], it is now a well-known fact that shoulder motion occurs in all the joints of the region simultaneously and each contributes its share to the completion of the movement. It is commonly believed that trapezius supports the shoulder and has the major role of rotating the scapula. Although Inman et al [1944] stated that trapezius supports the shoulder even at rest, there are several studies that reject this phenomenon [Fisk & Colwell, 1954; Bearn, 1961; Bagg & Forrest, 1986]. There are also a few studies that found trapezius to be a well-controllable muscle [Bearn, 1961; Palmerud et al., 1995].

2.5 Electromyography (EMG)

As was explained in Section 2.1, an action potential propagating down the axon of a motor nerve is transmitted chemically to the muscle fibers in the motor unit. This action potential gives rise to a shortening of the muscle fibers which in turn produces force; the signal resulting from the action potential in each muscle fiber of the motor unit is called the motor unit action potential (MUAP). However, in order to sustain a muscle contraction the motor unit must be repeatedly activated; hence resulting in a train of motor unit action potentials (MUAPT). The MUAPTs are, as a rule, completely asynchronous and this, along with the low pass dynamics of the muscle fibers, results in a smooth force output [Basmajian & De Luca, 1985]. The action potentials propagating along the muscle fibers give rise to an electrical signal which can be detected by surface or intramuscular electrodes. The resulting EMG signal, represents the gross electrical activity of the active motor units in the vicinity of the electrodes.

In human muscle tissue, the amplitude of the action potentials is dependent upon the diameter of the muscle fiber, the distance between the active muscle fiber and the detection site, and the filtering properties of the electrode [Basmajian & De Luca, 1985]. The amplitude of the EMG signal increases as the radius of the muscle fiber increases, and it decreases in approximately inverse proportion to the distance between the active fiber and the detection site. The action potential duration is inversely related to the conduction velocity of the nerve branch and muscle fiber [Basmajian & De Luca, 1985]. The waveform, and therefore the frequency spectrum of the action potentials, will be affected by the tissue between the muscle fiber and the detection site.

2.5.1 EMG Parameters

Several parameters of the EMG signal, such as root mean square (RMS) of the amplitude, median power frequency (MDPF), mean power frequency (MPF), the ratio of the RMS value of high-frequency components to the RMS value of the low-frequency components (RP), and peak frequency (PF) have been considered by researchers through the years. Stulen and De Luca [1981] compared the MDPF, MPF and RP. They pointed out that RP is the most sensitive parameter to changes in the conduction velocity of the muscle fiber. However, it was discarded due to several drawbacks such as having a non-linear relationship with changes in the conduction velocity and being dependent on the initial value of the characteristic frequency chosen to divide the spectrum. Stulen and De Luca [1981] also showed that MDPF and MPF have an equal linear sensitivity to the conduction velocity, with the MDPF about 20% less sensitive to signal to noise ratio than the MPF and concluded that MDPF is the most reliable parameter of EMG. In another study Hary et al [1982], concluded that MPF is the preferred parameter because of its lower standard deviation compared to that of MDPF and therefore smaller threshold for detecting statistically significant changes. Balestra et al. [1988] also compared the performance of MDPF and MPF parameters in both simulated EMG signals and EMG signals recorded from muscle during sustained muscle contraction. Their results showed that in both simulated and voluntary EMG signals, the MPF had a standard deviation at least 35% smaller than that of the MDPF regardless of the spectral estimation algorithm used.

2.5.2 EMG and Fatigue

The relationship of EMG parameters to muscle fatigue has been discussed for many years. It is commonly held that EMG behavior during the fatigue process is associated with a shift of its power spectrum toward lower frequencies and an increase in the RMS of the time signal. However, a difference in the trend of the power spectrum and the RMS shift in relation to the functional role of the muscle has been found [Moussavi et al, 1996]. Motor unit recruitment, motor unit synchronization, and a change in the conduction velocity of muscle fibers are three explanations that have been proposed to account for changes observed during a sustained, isotonic, and isometric contraction. According to Basmajian and De Luca [1985] the motor unit recruitment is unlikely to be responsible for the spectral changes of the EMG signal because amplitude increase and frequency shift have been observed in the first dorsal interosseous muscle during 80% of MVC and it is believed that at this contraction level, there is no further recruitment of motor units. Synchronization, which is defined as the tendency for motor units to discharge at almost the same time, has often been cited as the cause of both frequency shift and amplitude increase. However, synchronization of motor units has been reported to be more evident at the end of endurance time of contraction, whereas the frequency shift is more pronounced at the beginning of a contraction [Basmajian & De Luca, 1985]. Conduction velocity along the muscle fibers has been reported to decrease during a sustained contraction. To be more specific, using the model of Lindstrom et al [1970], the power spectrum of the EMG signal may be expressed as:

$$S(f) = (\tfrac{1}{v^2}).G(\tfrac{fd}{v}),$$

where υ is the conduction velocity of muscle, d is the distance between the detection surfaces of the bipolar electrodes and $G(.)$ is a mathematical model of the power spectrum of the EMG signal as a function of frequency and is implicitly dependent on many anatomical and experimental factors. $G(\,)$ may be expressed as

$$G(f) = \frac{F[\sigma_e^2(t)]}{E(k_j^{\,2}).k_a}.K,$$

where $E(\,)$ is the expectation operation, $F[]$ is the Fourier transform, k_a is the average firing rate of a motor unit train, σ_e^2 is the mean squared value of the EMG signal, k_j is a random variable, and K is a constant [Shwedyk et al, 1977].

From the above equations, it is possible to draw the following observations concerning the behavior of the spectrum:

- A decrease in the firing rates of motor units contributes to a shift of the power spectrum toward lower frequencies ??????.
- A decrease in conduction velocity causes the power spectrum to shift toward lower frequencies because the time-duration of the wave form increases as the conduction velocity decreases during sustained contraction and this would cause a simultaneous increase in the low-frequency components and a decrease in the high-frequency components.

There are a few hypotheses regarding the reason for the decrease in conduction velocity during a sustained contraction. They basically relate the decrease in conduction velocity to the changes of intramuscular pH, and explain it with biochemical changes in the

muscle fiber during a sustained contraction. However, the interaction between pH and conduction velocity is not firmly established [Basmajian & De Luca, 1985].

While the power spectrum shift of EMG with fatigue is a well established phenomenon, the RMS increase, however, is associated with ambiguity and controversy. Several investigators have studied the EMG signs of fatigue for trapezius muscle simultaneously with those of deltoid in an abducted or flexed arm position [Hansson et al, 1992; Gerdle et al, 1993]. While the results are similar, the interpretations are different and to some extent controversial. Since trapezius is considered to be a fatigue-resistant muscle with a predominance of type I muscle fibers, its less pronounced spectrum shift compared to that of deltoid is expected and has commonly been reported [Hansson et al, 1992; Oberg & Sandsjo, 1992; Gerdle et al, 1993]. However, Hansson et al. [1992] reported that the RMS value for trapezius showed a significant increase during an isometric fatigue process, the presented graphs showed that the deltoid's RMS remained constant or decreased. Some investigators have explained this difference by invoking the fact that the fiber type composition of the two muscles is different [Hansson et al, 1992; Gerdle et al, 1993]. However, this explanation raises some controversial aspects about EMG behavior during fatigue. A simple fact which has been ignored in previous research, is the functional role of the involved muscle, which may be a crucial determinant of the EMG signal characteristics. The hypothesis that the existence of such a relationship is an indicator of RMS behavior, has been studied in this research and is discussed in Chapter 4.

2.6 EMG Changes Associated with MPS

Although researchers have used EMG changes for many years as an indicator of muscle disorders, few of them have investigated the EMG signal associated with true MPS. Further, in research studies, probably because of ambiguity in the definition of MPS, subjects who have MPS have been mixed with fibromyalgic subjects and subjects with muscle spasm. This may explain the variable and to some extent conflicting, reported results.

Hagberg and Kvarnstrom [1984], investigated the changes of endurance time and EMG in ten subjects (aged 28-43) with a history of long-term shoulder-neck pain and no signs of inflammatory, rheumatic, or neuromuscular diseases. EMG signals were recorded by surface electrodes positioned over the descending part of trapezius muscle and by bipolar wire electrodes from the infraspinatus muscle bilaterally while the subjects held both upper limbs in a position of 30° shoulder flexion and 90° elbow flexion, and maintained the position to the limit of fatigue. RMS and MPF of the EMG signal were used as the indicator parameters. Results showed a significantly shorter endurance time on the painful side but no increase of motor unit activity was found on the painful side as compared to the pain-free side. EMG signs of fatigue developed faster on the painful side for the descending part of trapezius but not for the infraspinatus muscle.

In another study by Fricton et al [1985], significantly higher EMG activity than that in the normal muscle was reported for taut bands with trigger points. Using needle electrodes, Fricton and his group studied EMG recordings of the local twitch response in 16 subjects (mean age of 32) with long-term shoulder-neck pain due to active TPs in their

upper trapezius muscle, and compared these with recordings from the contralateral normal muscle in the same subjects. EMG recordings were made by initial snapping palpation of the muscle band within 5 cm of the needle electrode to elicit the local twitch response. The recordings were evaluated by visual scoring and spike counting. Results showed significantly higher motor unit activity upon snapping palpation, whereas the normal muscle fibers displayed minimal or no activity under the same conditions. This supports the notion that local twitch response is a valuable indicator for MPS. In contrast, Durette et al [1991], reported no difference between the EMG activity of normal muscles and muscles affected with MPS and fibromyalgia and therefore argued against the focal spasm theory of myofascial pain. However, their criteria for choosing subjects were somewhat different and they did not perform palpation during EMG recording as Fricton et al [1985] did. The results of Durette et al [1991], were consistent with those from a study by McBroom et al [1988], who investigated EMG in fibromyalgia syndrome. Yet another study [Hubbard & Berkoff, 1993] reported spontaneous EMG activity detected in trigger points when monopolar needle electrodes were inserted into the muscle within a 1 mm radius of the trigger points. Based on this result, Hubbard and Berkoff [1993] hypothesized that sympathetically stimulated intrafusal contraction causes an involuntary, low-grade but symptomatic muscle tension, which explains the autonomic symptoms associated with TPs.

More recently, Gogia and Sabbahi [1994] studied the EMG fatigue rate of anterior and posterior neck muscles in patients with osteoarthritis (OA) and compared it with those of normal subjects. They recorded EMG signals from the upper trapezius between C3 and

C6 bilaterally and also from the midpoint of the sternocleidomastoid muscles, while the subject was asked to perform an isometric contraction at 20%, 50% and 80% of MVC for 10 seconds. A significantly faster rate of fatigue was found in patients with OA of the cervical spine compared to normal subjects at the 50% and 80% of MVC contraction level. They correlated this result in the OA patients to the development of localized intramuscular ischemia at the higher force levels with pronounced accumulation of metabolites and reduced Ca+ ions. Since they found no difference in the initial median frequency between OA patients and normal subjects, therefore they rejected the possible change of fiber type composition in OA patients. However, they mentioned that the period of disease in those patients was short and therefore did not reject the possibility of change in fiber type composition in long-term as a result of the disease. In contrast, Oberg et al. [1992] found less pronounced spectral changes of EMG on the affected side of subjects with work-related myalgia; they studied EMG changes at different load levels in 11 female patients (mean age 37.6 years) with unilateral work-related myalgia of the trapezius muscle. They collected EMG signals from upper trapezius muscle and calculated normalized MPF and RMS of the EMG amplitude. At a 0 *kg* hand load, although the subjects experienced a feeling of fatigue in the region of the upper trapezius muscle, no decrease of MPF was observed, but a statistically significant increase of RMS on both affected (painful) and non-affected (pain free) sides was observed. At 1 *kg* and 2 *kg* hand loads, much more pronounced signs of fatigue (MPF decrease, and RMS increase) were observed. However, in all cases the fatigue signs were significantly more pronounced on the non-affected side. Oberg et al [1992] related this difference to inhibition due to pain.

individual movements of rotation, lateral flexion and flexion-extension of the head can be achieved. Movement of the suboccipital segment alone occurs between the occiput and the atlas, and between the axis and the third vertebra. The total range of flexion-extension of the occiput on the atlas is considered to be at most 15°, while lateral flexion is about 8°. The total range of motion of the combined superior and inferior segments is estimated to be 130° for flexion-extension; 45° for lateral flexion; and 80-90° for rotation to either side [Kapandji 1974].

Many joint models have been described in the medical literature; however, according to Kinzel and Gutkowski [1983], the most commonly used joint models are:

1. the one-DOF hinge or revolute joint,
2. the two-DOF planar joint,
3. the three-DOF spherical or ball and socket joint,
4. the two-DOF spherical joint,
5. the six-DOF spatial joint.

Because flexion-extension and rotation occur at the C1-C2 joint [Kapandji, 1974], the joint may be modeled as a two-DOF spherical joint, while the rest of the joints between C2-C7 vertebrae may be modeled as 3-DOF spherical joints, although the amount of motion at each joint is very limited.

2.7.2 Head-Neck Measurement

A means to measure both the range and pattern of motion in the head and neck region has been of interest to many researchers, particularly for physicians who need a

reliable and non-invasive tool to quantify changes in motion that might result from treatment. However, due to the complexity of head-neck movement and the lack of bony landmarks that can be used for reference points, little has been done in regard to developing a practical, accurate measurement of head-neck motion. The earliest studies of the neck's range of motion were based on visual determination [Cleveland 1918]. As described by Storms [1955], a ruler or measuring tape was used to measure the distance from the chin to the top of the sternum for flexion-extension, from the chin to the tip of the acromion for rotation, and from the ear to the tip of the acromion for lateral flexion. Fielding [1957], and Kottke and Lester [1958], used cineroentgenography to measure flexion-extension. Goniometry has also been used by many researchers to measure cervical spine motion [Moore 1949; Ferlic 1962; Newell and Nichols 1965; Tucci et al, 1986]. Depending on the type of goniometer utilized, different arrangements were used to position the goniometer on the top of the head. Tucci et al, [1986] used a gravity goniometer with a head adapter and compared its readings to those taken with a universal goniometer. Compared to a universal goniometer, they reported much higher intraclass correlation coefficients when two different examiners used the gravity goniometer and therefore concluded that the gravity goniometer is more accurate and reliable. Chao et al, [1989] introduced a method of measuring head-neck motion utilizing low-frequency magnetic field coupling theory to determine the location and orientation of a 'sensor' compared to a reference as 'source'. The sensor was placed on a subject's forehead and the source was fastened on the trunk which was immobilized in a chair. More recently, Alund and Larsson [1990] used electrogoniometry to measure head-neck motion clinically

and compared their results with those from gravity goniometers. Their results are compared with the results of this study and presented in Chapter 4.

The disadvantages of the above mentioned methods may be summarized as follows:

- lack of accuracy in the visual determination method;
- radiation exposure, expense and required expertise for interpretation in the roentgenography method;
- inaccuracy of goniometers in general.

Although relatively accurate assessment of cervical motion may be obtained by the gravity goniometer, securing the device to the top of the subject's head with belts may not be desirable for patients, especially those with stiff necks. Also the above mentioned methods measure the head-neck motion in only one plane at a time. Since vertebral motion is coupled, e.g., lateral flexion is accompanied by rotation [Panjabi & White, 1980], measurement of composite head-neck motion is preferable for studying the pattern of motion, in particular in patients with cervical spine problems.

2.9 Summary

Each muscle contains up to a few hundred motor units. Each motor unit consists of all muscle fibers that are innervated by a single cell in the spinal cord by one axon. In order for a muscle to contract, nerve impulses (action potentials) need to be transmitted to muscle fibers causing the contractile apparatus within the muscle cell to change the

configuration of actin and myosin molecules. As a result of this change, the actin and myosin filaments bind to each other and the crossbridge of myosin to actin is formed. After the crossbridges are formed, the stored energy in the myosin's head, makes the bridge to rotate forward, while it is still attached to actin. Therefore, these filaments slide along each other and cause muscle contraction. During the process of muscle relaxation, energy is required to separate the actin and the myosin filaments.

Sustained and strong contraction of a muscle leads to the state of muscle fatigue. In extreme degrees of muscle fatigue, there is an energy crisis in the muscle. Therefore the binding of the actin and myosin filaments may remain rigid for many minutes even without an action potential as a stimulus.

It has been proposed that trauma or over-load use of a muscle without sufficient relaxation time may lead to the development of myofascial trigger points, which are most commonly found in trapezius muscle. Myofascial pain syndrome due to trigger points has some well-known characteristics, such as local twitch response, referred pain and general weakness of the affected muscle.

Electromyography (EMG) has been used to monitor muscle activity during both dynamic and sustained contraction. The fact that the EMG spectrum changes with fatigue during sustained and isometric contraction is well-known. Since muscles with MPS have been shown to be weaker than normal muscles, one of the objectives of this research was to study the EMG features of trapezius muscle (the most common affected muscle with myofascial TPs) during a fatigue process in patients with trapezius myalgia due to myofascial trigger points and compare the features with those of healthy individuals.

In general, TPs restrict the normal range of motion. In particular, TPs in upper trapezius cause restriction in head-neck range of motion. Therefore, another objective was to measure head-neck range of motion in patients before and after treatment and to compare the results to those of healthy individuals.

CHAPTER 3

MATERIALS AND METHODS

3.1 Research Design

To investigate changes as a result of treatment, a repeated measures design [Portney & Watkins, 1993] was used. To compare the data of intervention and control groups, a nonequivalent pretest-posttest control group design [Portney & Watkins, 1993] was used.

3.2 Research Hypotheses

This research aimed to test the following hypotheses:

- EMG Fatigue pattern of myalgic muscles is different from that of healthy muscles.
- There is a change in myalgic muscles after treatment.

To test the first hypothesis, EMG fatigue patterns of trapezius and deltoid in healthy subjects and patients were compared. The second hypothesis was considered and tested from three aspects: electrical changes using EMG, biomechanical changes using head-neck motion and subjective changes using subjective measurements such as pain and patients' perception of their performance.

consent to participate in the study. The Control group consisted of a sample of convenience; they were healthy volunteer subjects with no history of active TPs in upper trapezius or other shoulder girdle muscles.

Subjects in both groups were between the ages of 18 and 55 years. The mean age of the subjects in the intervention group was 43 ± 9 years, while it was 28 ± 8 years in the control group.

Subjects in the intervention group were required to participate in experiments at four different sessions: one within 10 days before the first treatment by the physiatrist, one within 10 days after the first treatment, another at 6-8 weeks and lastly at 12 weeks after the first treatment. These test sessions were designated M1, M2, M3 and M4. Subjects in the control group were tested three times with the intervals of three weeks between the sessions.

3.5 EMG Recording

Decisions about the instrumentation to be used while recording the EMG signal include the choice of electrodes, amplifiers, filters, recording and display devices. Since one of the objectives of this investigation was to study the EMG activity of trapezius and deltoid muscles in patients with myofascial TPs and also because these muscles are surface muscles, self adhesive silver-silver chloride surface electrodes were used to record EMG signals. After skin preparation by rubbing alcohol to reduce skin resistance, the electrodes were placed on middle, posterior and anterior portions of deltoid (MD, PD and AD, respectively) and upper, middle and lower portions of trapezius (UT, MD, and LT,

respectively). Figure 3.1 shows the electrodes' placement. For technical reasons, such as eliminating noise from the vicinity of the detection area, the EMG electrodes were used in a bipolar configuration. The EMG signal was amplified differentially to prevent artifacts and was filtered by a band-pass filter with 10 and 500 *Hz* cutoff frequencies. It was simultaneously digitized at 1 *kHz* sampling rate and stored in the computer.

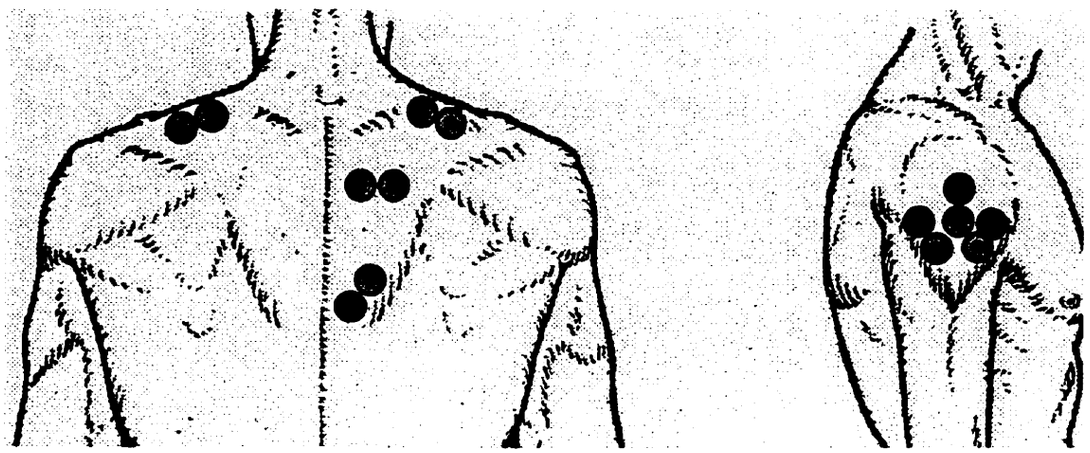

Figure 3.1 Electrodes' placement. Reference electrodes are not shown.

3.6 Test Positions for EMG Recording

Two test positions were designed for the EMG experiments:

Position A- The subjects were asked to hold their left and later their right upper limb in 90° shoulder abduction, 0° elbow flexion, and 90° forearm pronation until the limit of fatigue. Meanwhile the EMG signals from upper trapezius and from the middle, posterior and anterior portions of deltoid were amplified, digitized and stored in the computer. The same experiment was repeated in the same order while the subject held a 1kg load in

his/her hand. There was a 10 minute rest period between each trial. To ensure that the subject did not lower his/her arm as a result of fatigue, a small marker was placed just under the subject's hand so that the subject consciously tried to stay above the marker.

Position B- After the two trials in position A followed by a 10 minute rest interval, subjects were asked to elevate their shoulders and retract as much as possible and to maintain the position until fatigue. In this position, the subject was asked to watch his/her position on a monitor and avoid any motion. The EMG signals were recorded from middle deltoid, upper, middle and lower portions of trapezius muscle, digitized and stored in the computer. Figure 3.2 shows test positions.

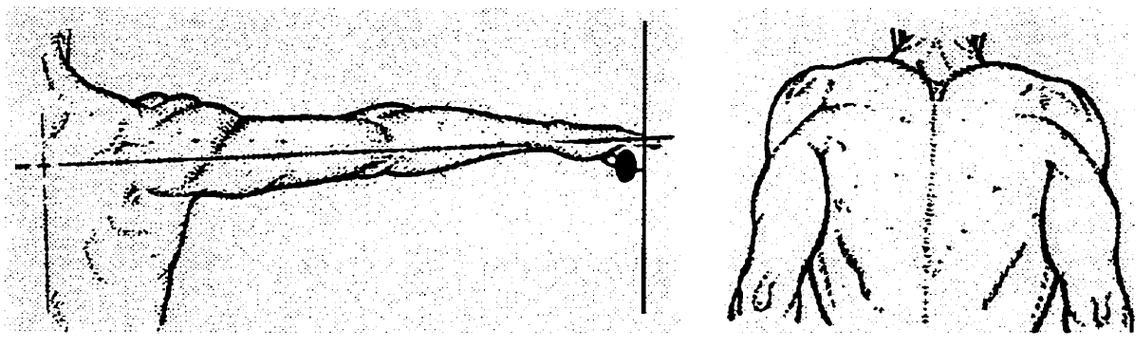

(A) (B)

Figure 3.2 Test positions A and B.

3.7 EMG Feature Selection

The EMG signal during an isometric and isotonic contraction for a short period of time may be considered as a stationary signal. However, the signal's statistics change with fatigue. Since fatigue is a slow process that does not change the statistics of the EMG

signal in less than, i.e. 10 s, it is a common practice to observe EMG signal through 0.5 or 1 s window. Therefore, to estimate the power spectrum of EMG, the raw data was segmented into 1 s segments with a 50% overlap between the segments. To minimize the bias of power spectrum estimator, the optimum moment energy window [Papoulis, 1977] was applied for segmentation. For every 1 s segment, the time signal's RMS value was calculated. Then the power spectrum was determined by estimating the autocorrelation function and using a spectral hamming window with a length of 128 samples for each segment [Appendix A]. Both median and mean power frequencies (MDPF and MPF) were estimated from the power spectrum. MPF was chosen as the preferred parameter due to its smaller standard deviation. The statistical characteristics of MDPF and MPF were also studied. It is shown theoretically that MPF is an asymptotically unbiased estimator and that the MDPF estimator is convergent in the probability sense [Appendix B]. Since the power spectrum of the EMG signal is considered to be band limited, it may also be concluded that MDPF estimator is convergent in a mean square sense [Jenkins & Watts, 1968].

The MPF and RMS trends of EMG signals from MD and UT muscles were analyzed further. From the MPF trend of the EMG signal, an average of the first 10 s and the last 10 s of the trend were calculated and the ratio between these two numbers was used as indicator of the total shift of MPF during the fatigue process. The same procedure was used to determine the total shift of the RMS. The slope of MPF versus time, or the so-called "fatigue rate", was also calculated. These parameters were the main EMG features that were compared between the sessions and groups. In order to be able to

average between signals with different lengths due to different endurance times, the MPF and RMS trends were each averaged for every 5% of the total endurance time, normalized by the maximum value, and were saved in the separate files. The MPF and RMS trends of the other recorded signals (AD, PD, MT and LT) were also considered for further study of the fatigue pattern of trapezius in relation to its functional role, in particular in healthy subjects.

To summarize, the following parameters of the EMG signals obtained from MD and UT muscles, were studied and compared between and within groups:

- total shift of MPF;
- total shift of RMS;
- slope of MPF (fatigue rate);
- endurance time.

3.8 Head-Neck Model

The human neck consists of seven vertebrae. If the height of each cervical vertebra is assumed to be approximately 7.5 *mm* and each of the disks to be 3 *mm* thick [Kapandji, 1974], the length of an average neck can be calculated to be approximately 7.1 *cm* in total. During maximum neck excursion, the disk thickness may change slightly. However, because of the small number of disks in the cervical column, the difference between the neck's length in upright and maximum excursion positions is negligible. Therefore, it is possible to model the neck as a solid tube rotating in a ball and socket joint. Although actual head-neck movement is very complex, by considering only the resultant motion a

simple model can be designed that assumes the combined head and neck joints act as a ball and socket joint with three DOF.

This model can be used to determine head-neck motion by defining three coordinate systems: CS_0 as the absolute reference system, CS_1 for head-neck and CS_2 for trunk. The coordinate system for the trunk is needed to eliminate the effect of shoulder girdle excursion during head-neck motion. Coordinate systems CS_1 and CS_2 rotate with head-neck and trunk movement, respectively. The axes of CS_1 and CS_2 can be defined so that their rotational Euler angles with respect to CS_0 correspond to the absolute motion of the head-neck and trunk with respect to the reference system. Therefore the above relationship can be written as

$$[CS_1] = [T_0].[CS_0],$$

$$[CS_2] = [T_1].[CS_0],$$

where T_0 and T_1 are transformation matrices. Then relative motion of the head-neck with respect to the trunk can be calculated as:

$$[CS_1] = [T_0].[T_1]^{-1}.[CS_2] \Rightarrow [CS_1] = [T].[CS_2], \qquad (3.1)$$

where the transformation matrix, $[T]$, is defined as

$$[T] = \begin{bmatrix} \cos\varphi\cos\psi - \sin\varphi\sin\theta\sin\psi & \sin\varphi\cos\psi + \cos\varphi\sin\theta\sin\psi & -\cos\theta\sin\psi \\ -\sin\varphi\cos\theta & \cos\varphi\cos\theta & \sin\theta \\ \cos\varphi\sin\psi + \sin\varphi\sin\theta\cos\psi & \sin\varphi\sin\psi - \cos\varphi\sin\theta\cos\psi & \cos\theta\cos\psi \end{bmatrix} \qquad (3.2)$$

The Euler angles ϕ, θ, ψ are the rotation of coordinate system CS_1 with respect to coordinate system CS_2. Note that the above transformation matrix is produced by the following rotation sequence: Z axis by ϕ, Y axis by θ and then X axis by ψ.

In practice the coordinate systems CS_1 and CS_2 are defined by a set of seven reflective markers as shown in Figure 3.3.a. Anatomical landmarks are used to define marker placement:

- marker 1 is placed on top of marker 2 which is located at the apex of the head. The apex is defined as the intersection of the curve between inion and nasion and the curve between the tragi of right and left ears;
- marker 3 is oriented to the right side of marker 2 perpendicular to the vector between markers 1 and 2 and in line with the tragal curve;
- marker 4 is placed over the jugular notch of the sternum;
- marker 5 is placed over the sternal angle;
- markers 6 and 7 are placed over the left and right acromio-clavicular joints, respectively.

With the above marker placement, the orthogonal axes of the head-neck and trunk coordinate systems are defined as:

CS_1: Head-neck orthogonal axes:

$$\vec{z}_1 = \frac{\vec{v}_{21}}{|\vec{v}_{21}|}$$
$$\vec{y}_1 = \frac{\vec{v}_{21} \times \vec{v}_{23}}{|\vec{v}_{21} \times \vec{v}_{23}|} \qquad (3.3)$$
$$\vec{x}_1 = \vec{y}_1 \times \vec{z}_1$$

CS_2: Trunk orthogonal axes:

$$\vec{z}_2 = \frac{\vec{v}_{54}}{|\vec{v}_{54}|}$$
$$\vec{y}_2 = \frac{\vec{v}_{54} \times \vec{v}_{67}}{|\vec{v}_{54} \times \vec{v}_{67}|} \qquad (3.4)$$
$$\vec{x}_2 = \vec{y}_2 \times \vec{z}_2$$

where the notation $\vec{v}_{ab}$ denotes a vector from marker a to marker b and $\times$ is the cross product operator. The directions of the vectors in the two coordinate systems are shown in Figure 3.3.b.

From Equation 3.1, the relationship between the head-neck and the trunk coordinate systems can be rewritten as:

$$\begin{bmatrix}\vec{x}_1 & \vec{y}_1 & \vec{z}_1\end{bmatrix}^T = [T].\begin{bmatrix}\vec{x}_2 & \vec{y}_2 & \vec{z}_2\end{bmatrix}^T, \tag{3.5}$$

A simple matrix calculation on Equation 3.5, gives:

$$[T] = \begin{bmatrix} \langle \vec{x}_2.\vec{x}_1 \rangle & \langle \vec{x}_2.\vec{y}_1 \rangle & \langle \vec{x}_2.\vec{z}_1 \rangle \\ \langle \vec{y}_2.\vec{x}_1 \rangle & \langle \vec{y}_2.\vec{y}_1 \rangle & \langle \vec{y}_2.\vec{z}_1 \rangle \\ \langle \vec{z}_2.\vec{x}_1 \rangle & \langle \vec{z}_2.\vec{y}_1 \rangle & \langle \vec{z}_2.\vec{z}_1 \rangle \end{bmatrix}, \tag{3.6}$$

where $\langle .,. \rangle$ is the inner product operator. Equations 3.5 and 3.6 form nine non-linear equations, from which the Euler angles, φ, θ, ψ, must be found, making the system redundant. Using the method presented in Appendix C, the unique and correct solution of the above equations can be found. Note that the defined coordinate systems yield Euler angles that correspond directly to the anatomical angles of head-neck movement, i.e., the angles φ, θ, ψ represent rotation, flexion-extension and lateral flexion, respectively. The operation of Euler angle calculation program is presented in Appendix D.

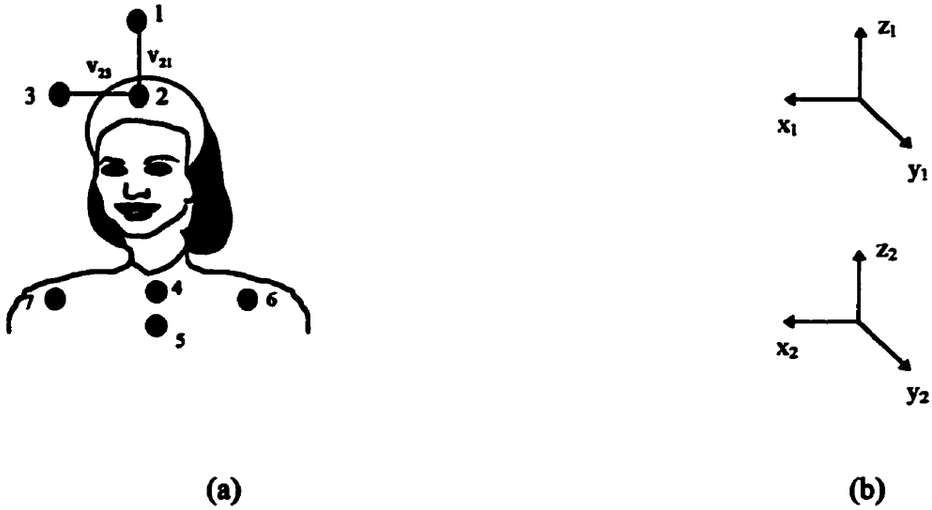

Figure 3.3 (a) Location of the markers (b) Head and trunk orthogonal axes.

3.9 Head-Neck Measurement

The ability of the head-neck model to yield Euler angles that correspond directly to the anatomical angles of head-neck movement was confirmed by developing a simulation program to produce and plot head-neck movement based on the proposed model and an input of an arbitrary set of angles. The model was then used to calculate the angles of head-neck motion of healthy individuals and also of patients. Seven light-weight (less than 10 *g*), reflective markers were attached to the body as previously described. In order to prevent sliding of the markers on the hair, subjects were required to wear a tight-fitting, light-weight nylon cap to which reflective markers 1, 2 and 3 were taped securely. Three orthogonally placed cameras were used to capture the motion data on video tape; cameras were calibrated before each test session. The subject was seated within the visible area of

cameras and was asked to slowly flex-extend, side flex and rotate the head and neck to either side. Each motion was repeated three times. The motion was video taped and the marker coordinates were digitized using UM^{2}AS. From the location of the markers, the unit vectors for the head-neck and trunk coordinate systems were calculated from Equations 3.3 and 3.4 and the anatomical angles of motion were then calculated by the method described in Appendix C. In order to test the reproducibility of the method, each healthy subject was asked to repeat the experiment three times with the sequence of motions randomized between trials. The patients were asked to perform the same experiment as that done by the healthy individual. However as was described in Section 3.2, there were four test sessions for patients. A one way repeated measures ANOVA was used to test the statistical significance difference between and within the groups. In all instances, the probability of being wrong when asserting that a true difference exists, p value, was less than 0.05.

3.10 Subjective Measurements

Aside from the objective measurements and data, two subjective measurements were also used: pain measured with a visual analog scale (VAS) and perception of disability measured with the Canadian Occupational Performance Measure (COPM).

Pain Data: A score was generated for each visual analog pain scale [Huskisson, 1974]. A VAS is a 10 cm line anchored at the lower end by "No Pain" and at the upper end by "Intolerable Pain". The subject placed a mark on the line to indicate the amount of pain felt.

COPM Data: The COPM is a standardized instrument that uses a 10-point scale to quantify subject-identified problem areas in daily functioning and generates a score based on the importance of the task to the subject and the subject's satisfaction with his/her performance [Law et al, 1990]. Two scores (Performance, Satisfaction) are generated using the COPM instrument. The performance score (PF) is obtained by multiplying the subject's rating of importance of each identified activity with his/her rating of ability to perform the activity; the resultant values are added and divided by the number of rated activities. The satisfaction score is obtained by multiplying the importance rating by the subject's rating of satisfaction with ability to perform the activity, adding the resultant values and dividing by the number of rated activities.

The Friedman test, the nonparametric equivalent of the repeated measures analysis of variance (ANOVA), was used to compare the subjective measurements before and after treatment.

3.11 Protocol (Summary)

To study the EMG and MPS relationship, and to investigate the effect of treatment on TPs, the following protocol was used in this thesis.

Subjects: A total of eighteen subjects participated (9 in the Intervention group, 9 in the Control group) as was described in Section 3.2.

Method: To compare objective measures a one way repeated measures ANOVA was used for the session data from each group of intervention and control subjects. Both a two

way ANOVA and a t-test were used to compare results between the two groups. Dependent variables were the total shift of MPF and RMS, fatigue rate, endurance time of the EMG signal and range of motion (ROM) of the head-neck measured in degrees. Since the subjects in the Intervention group were restricted to those that did not have TPs in their deltoid or arm muscles, the motion measurement was also limited to head-neck motion. To compare subjective measures within the intervention group, a Friedman test was used. Dependent variables were pain scores from the VAS, and disability scores from the COPM. The independent variable in both objective and subjective analyses was the standard MPS treatment protocol of the medical specialist in physical medicine and rehabilitation who routinely treated patients with MPS. Treatment included needling and 1% xylocaine injection, spray and stretch, hydrocollator hot packs, and a self stretch program.

Instruments:

1. EMG - self-adhesive surface electrodes were used in a bipolar configuration. The electrodes were connected to multi-channel amplifiers with the output displayed on an oscilloscope for visual inspection. The analog signals from the amplifier were conveyed to a 16 channel NT A/D board to be digitized and stored in a pc586 computer for subsequent analysis.
2. Range of Motion - UM^{2}AS was used to track the motion and the head-neck model presented in Section 3.6, used to calculate the head-neck angles of motion.
3. Pain Measurement - A VAS was used to measure the subjective experience of pain.

4. Disability Measurement - The COPM was used to quantify the subjective experience of disability.

Procedure: There were four (M1-M4) test sessions for subjects in the intervention group and three test sessions for those in the control group at the same time intervals excluding session M2 (described in Section 3.2). Demographic data from patients were gathered prior to M1. Surface electrodes for EMG were placed at defined positions over the upper, middle and lower portions of trapezius, middle, posterior and anterior portions of deltoid muscles. EMG signals were recorded while the subject performed the test positions A and B (described in Section 3.4) held until extreme fatigue was felt. A 10 minute rest was interposed between each trial to allow the muscles to recover and to minimize the possibility of post-exercise discomfort. The sequence of EMG recording was not randomized and was fixed for all subjects.

Reflective markers for video motion analysis were attached to the head and trunk as explained in Section 3.6. Subjects were required to flex/extend, side flex and rotate their head and neck as far as possible while being videotaped; no assistance was given to increase the extent of joint range. To decrease the possibility of bias, the motion sequence was randomized.

For the Intervention group the COPM was administered and information about activity levels was documented before M1, M2, M3 and M4; pain level was measured before and after each test session.

Data Analysis:

- EMG Data: After testing, the total shift of the mean power frequency and RMS of the time signal, fatigue rate and the endurance time of each experiment were extracted (described in Section 3.5). Therefore, there were four sets of EMG values (at M1, M2, M3 and M4) for each subject in the intervention group and three sets of values for the control group.
- Motion Data: The video tapes of motion were digitized and angles of head-neck motion were calculated based on the model presented in Section 3.6. There were four sets of angle values (at M1, M2, M3 and M4) for each subject in the intervention group and one set for those for the control group.
- Pain Data: A score was generated for each pain VAS administered according to the protocol of Huskisson [1974]. Three pain scores were generated at each test session - pain level before the fatigue task (p1), pain level after the fatigue task (p2) and the difference between p1 and p2 (p2-p1)). There were four sets (at M1, M2, M3 and M4) for each pain score.
- COPM Data: Two scores (Performance, Satisfaction) were generated at each measurement session. Again, there were four sets (at M1, M2, M3 and M4) for the performance and satisfaction scores.

Statistical Analysis: After data extraction, a two-way (Treatment, Session) repeated measures Analysis of Variance (ANOVA) was used for each of the MPF and the range of motion parameters to test the hypothesis that there was a difference between sessions as a

result of treatment. Pain scores and endurance time were tested using a one-way (Session) repeated measures ANOVA; COPM scores were tested with a Friedman test [Hassard, 1991]. A Spearman rank correlation coefficient was calculated to determine if there was a significant relationship between EMG features, range of motion and subjective pain and disability data. In all instances $p \leq 0.05$. Figure 3.4 shows a schematic flowchart of the research procedure.

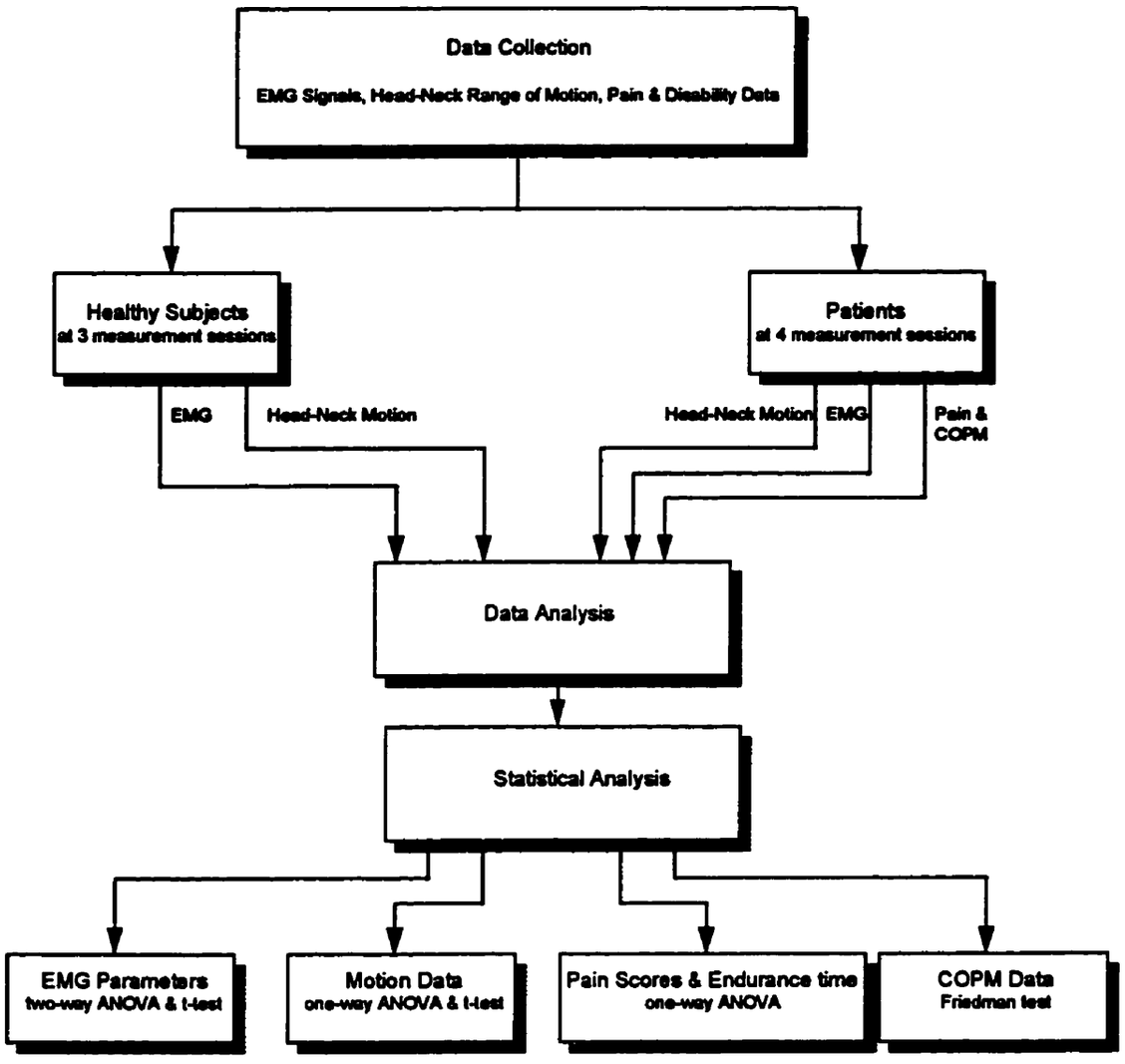

Figure 3.4 Schematic presentation of the research procedure

CHAPTER 4
RESULTS AND DISCUSSION

4.1 Introduction

This chapter considers the results in three sections, each followed by a discussion. The EMG results are considered first, followed by the biomechanical results which are discussed in Section 4.3. Lastly, the subjective results of patients are presented in Section 4.4. The last section in this chapter presents an overview which integrates the results of the three sections.

4.2 EMG Results

None of the selected parameters were significantly different between the trials of healthy subjects at different sessions. Therefore, the average of each of the selected parameters of healthy subjects across the three different sessions was calculated and compared with that of the patients. In all cases either a t-test or repeated measures ANOVA were used to test for significance.

Overall, there was a significant difference between the fatigue pattern of healthy and myalgic muscles. In healthy muscles, there was an obvious plateau at the end of MPF shift toward lower frequencies when the muscle was acting as a prime mover and at a low contraction level. This plateau was completely absent in the myalgic muscles. Figure 4.1

shows a typical MPF trend of middle deltoid of a healthy subject in comparison to that of middle deltoid on the affected side of a patient in position A, 0 kg hand load.

In general, there was a significant difference between the endurance time of healthy subjects and patients at the low contraction level (0 kg hand load). At the high contraction level (1 kg hand load) the endurance time of healthy subjects was greater than that of patients but the difference was not statistically significant. The endurance time of patients increased after treatment in both test positions. However, its increase was statistically significant only for position B. The summary of these results is listed in Table 4.1.

The results of the selected EMG parameters are discussed in more detail in the following sub-sections.

	M1-M2-M3-M4	HS - P_M1	HS - P_M2	HS - P_M3	HS - P_M4
Exp.A - 0 kg	$p = 0.09$	277 - 152 *s* $p = 0.001$*	277 - 156 *s* $p = 0.006$*	277 - 180 *s* $p = 0.003$*	277 - 167 *s* $p = 0.0006$*
Exp.A - 1 kg	$p = 0.19$	122 - 90 *s* $p = 0.068$	122 - 107 *s* $p = 0.39$	122 - 101 *s* $p = 0.16$	122 - 98 *s* $p = 0.08$
Exp B	M1-M4 $p = 0.009$* M1-M3 $p = 0.01$* M1-M2 $p = 0.08$	477 - 95 *s* $p < 0.001$*	477 - 127 *s* $p < 0.001$*	477 - 155 *s* $p < 0.005$*	477 - 180 *s* $p < 0.003$*

Table 4.1 Summary of endurance times of healthy subjects and patients at different sessions. The numbers correspond to the mean value of endurance time for each group in seconds. Legend: HS and P_M# correspond to healthy subjects and patients at session M1 to M4, respectively. * refers to statistical significance.

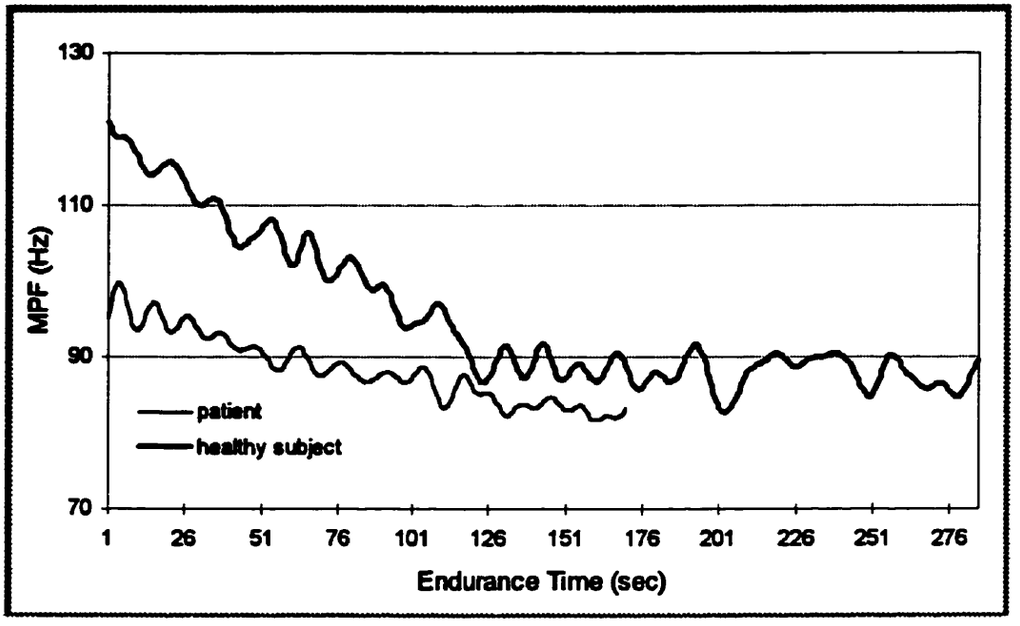

Figure 4.1 The MPF shift toward lower frequencies of middle deltoid of a healthy subject and of a patient during position A, 0 kg.

4.2.1 Mean Power Frequency (MPF) Shift

Healthy Subjects

MPF values of both middle deltoid and upper trapezius showed significant changes during fatigue in position A ($p < 0.01$), while the MPF shift of middle deltoid was significantly greater compared to that of upper trapezius ($p < 0.002$). Figures 4.2.a and 4.2.b show the MPF shifts, averaged for the nine subjects, of middle deltoid and upper trapezius for the low contraction level in position A.

The MPF shifts of the anterior and posterior portions of deltoid were significantly less than that of the middle part for both loading conditions in position A.

For position B, the MPF of upper and middle portions of trapezius showed significant shifts toward lower frequencies ($p <0.03$), while that of the lower trapezius was not significant ($p > 0.1$). Figure 4.2.c shows the MPF trend of upper trapezius during position B, averaged across the nine subjects.

Patients

The MPF shifts of middle deltoid and upper trapezius in position A were significantly less than those of healthy subjects ($p < 0.04$). However, the MPF shift of middle deltoid was more pronounced after treatment compared to that before treatment.

The MPF shift of upper trapezius in position B was not significantly different between the patients and the healthy subjects or between different measurement sessions M1 to M4. It was lower in patients than in healthy subjects.

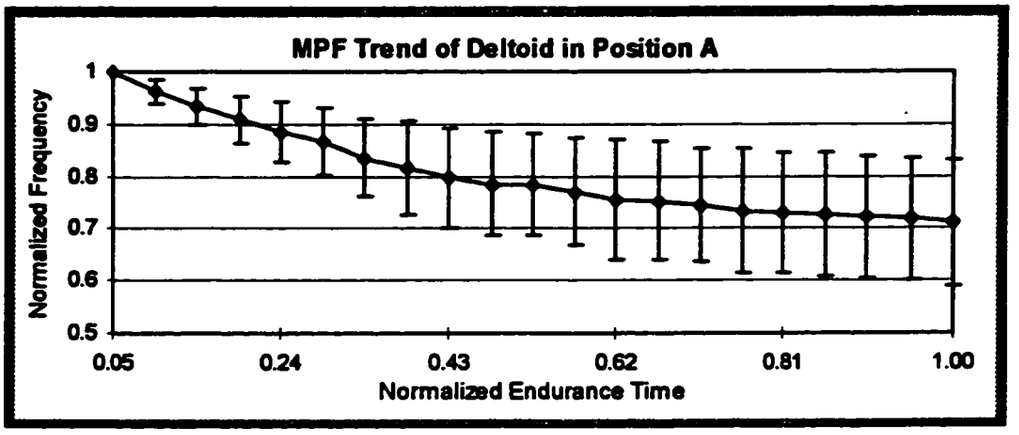

(a)

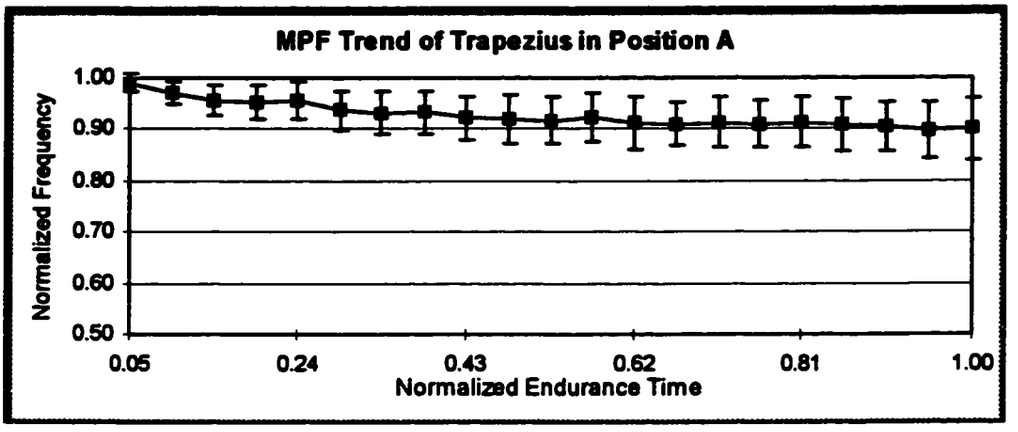

(b)

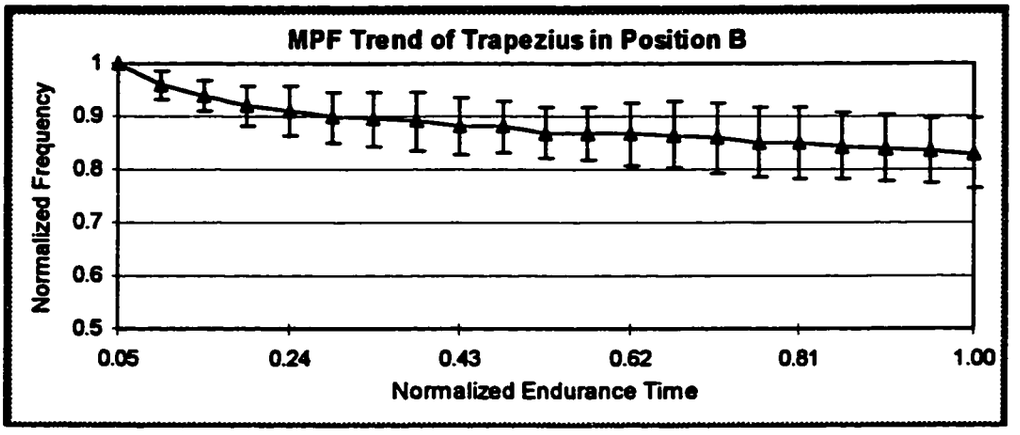

(c)

Figure 4.2 The mean MPF trend of right middle deltoid and right upper trapezius of healthy subjects in positions A (0 kg hand load) and B. The error bars show the standard deviation.

4.2.2 Root Mean Square (RMS)

Healthy Subjects

In position A, for both contraction levels, the RMS of upper trapezius increased significantly ($p < 0.01$) and almost linearly in all trials. Figure 4.3.b shows the RMS of the upper trapezius in position A, 0 kg. In contrast, the RMS values of middle deltoid, which was acting as a prime mover in position A, showed a different pattern; in most cases there was a decrease followed by an increase. On average, there was approximately a 10% decrease over time (Figure 4.3.a). The RMS of the posterior and anterior portions of deltoid remained almost constant in all trials.

For position B, in which it was acting as a prime mover, the RMS of upper trapezius showed a similar pattern to that of middle deltoid in position A. On average, the RMS decreased slightly but its decrease was not significant ($p > 0.4$). Figure 4.3.c shows the RMS trend of upper trapezius in position B.

The RMS behavior of middle trapezius for position B was variable between the subjects, probably due to the fact that it was hard for individuals to control the amount of shoulder retraction. This portion of the muscle acts as a prime mover for shoulder retraction, while it is a stabilizing synergist for shoulder elevation. The RMS of the lower portion of trapezius either showed no change or increased slightly for position B, possibly because this portion of the muscle has little functional role in shoulder elevation and retraction.

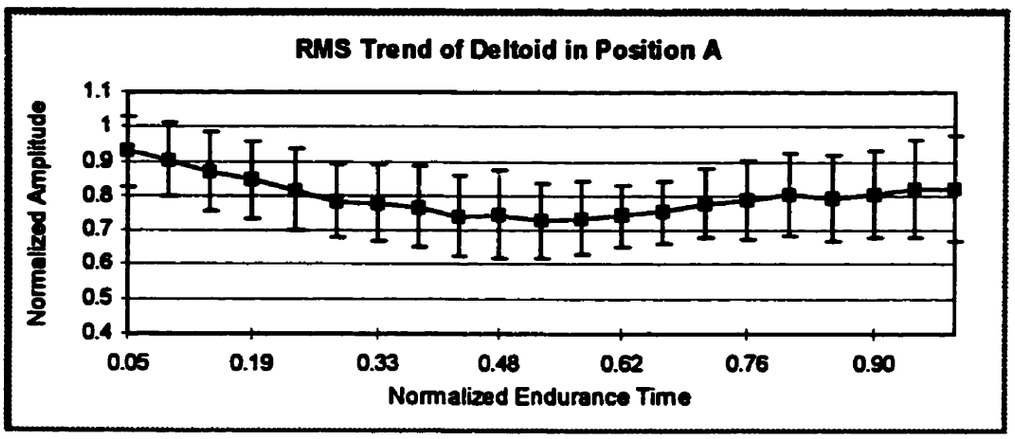

(a)

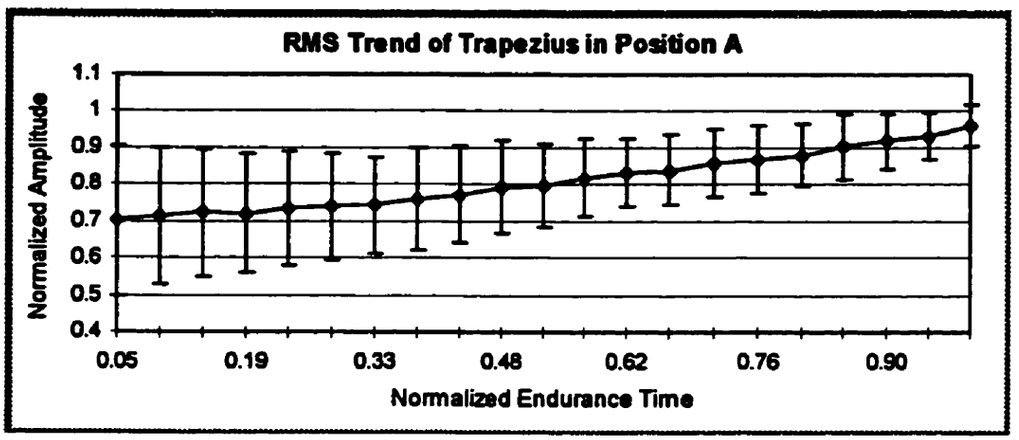

(b)

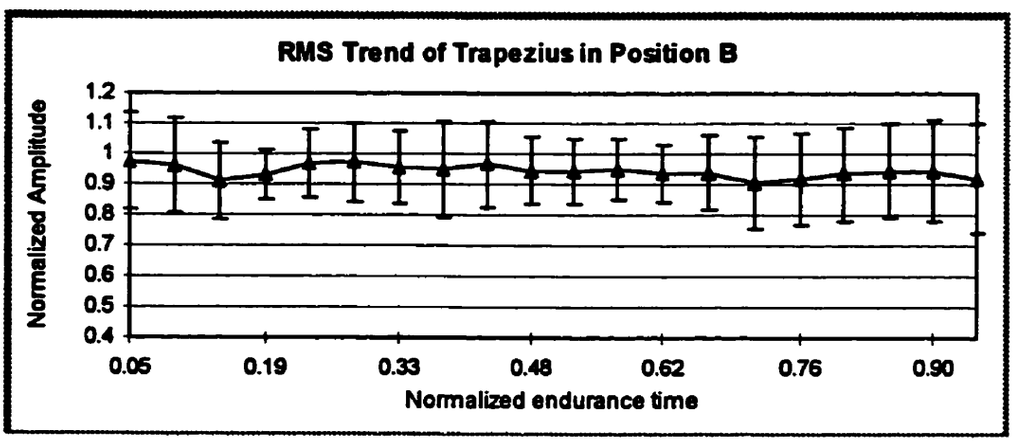

(c)

Figure 4.3 The mean RMS trend of right middle deltoid and right upper trapezius of healthy subjects in positions A (0 kg hand load) and B. The error bars show the standard deviation between the subjects.

Patients

In general, the initial activity of trapezius was significantly higher before treatment, compared to that in healthy subjects ($p < 0.01$). In position A, there was a difference between the upper trapezius' RMS trend compared to that of healthy subjects; this difference remained even after treatment. On average, the increase of upper trapezius' RMS of patients was less than that of healthy subjects (Figure 4.4). This difference was statistically significant ($p < 0.04$) for high level contractions in position A (1 kg hand load). It is worth noting that in this position (A), where the upper trapezius acted as a stabilizer, the RMS value increased in all healthy subjects. This increase was not only less pronounced in patients, there was even a decrease in some of the patients.

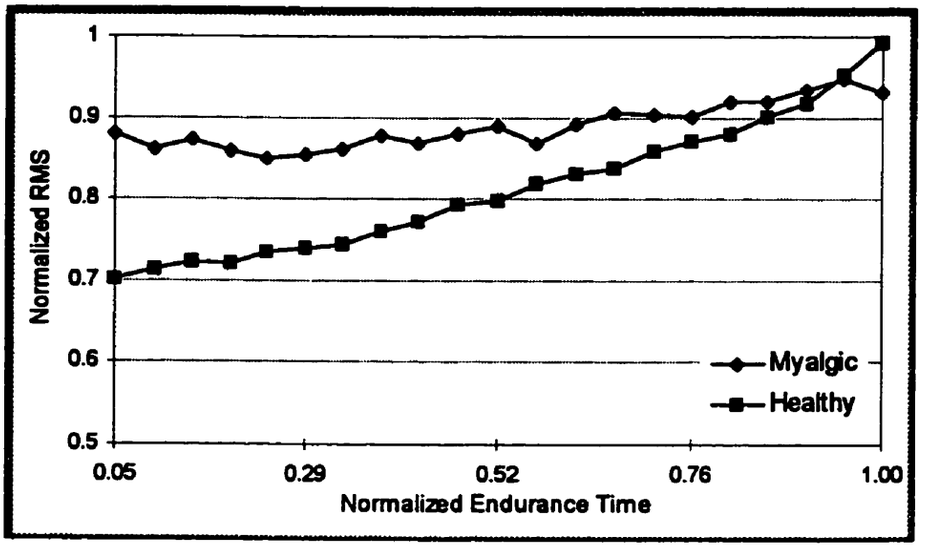

Figure 4.4 The mean RMS trend of upper trapezius of patients before treatment and healthy subjects for position A, 0 kg hand load.

4.2.3 Fatigue Rate (Slope of Mean Power Frequency Over Time)

Healthy Subjects

The fatigue rate (the slope of MPF) of the middle deltoid was significantly greater than that of the upper trapezius for both contraction levels in position A ($p < 0.0013$). In the case of the upper trapezius, its fatigue rate when acting as a prime mover (position B), was faster than that when acting as a stabilizer (position A).

Patients

In comparison to that of healthy subjects, the patients' fatigue rate of upper trapezius in position A, was faster. However, the difference was not statistically significant ($p > 0.2$). For position B, the fatigue rates of upper trapezius at sessions M1 and M2 were significantly faster than those in healthy subjects ($p < 0.02$). However, the fatigue rate decreased significantly ($p < 0.021$) in sessions M3 and M4. Figure 4.5 shows the averaged fatigue rate of healthy subjects and that of patients in the four sessions.

The fatigue rate of middle deltoid for position A also decreased significantly ($p < 0.01$) in sessions M3 and M4 compared to that in session M1. In general the fatigue rate of middle deltoid was faster in patients compared to healthy subjects; however, the difference was not statistically significant ($p > 0.22$) in any of the measurement sessions.

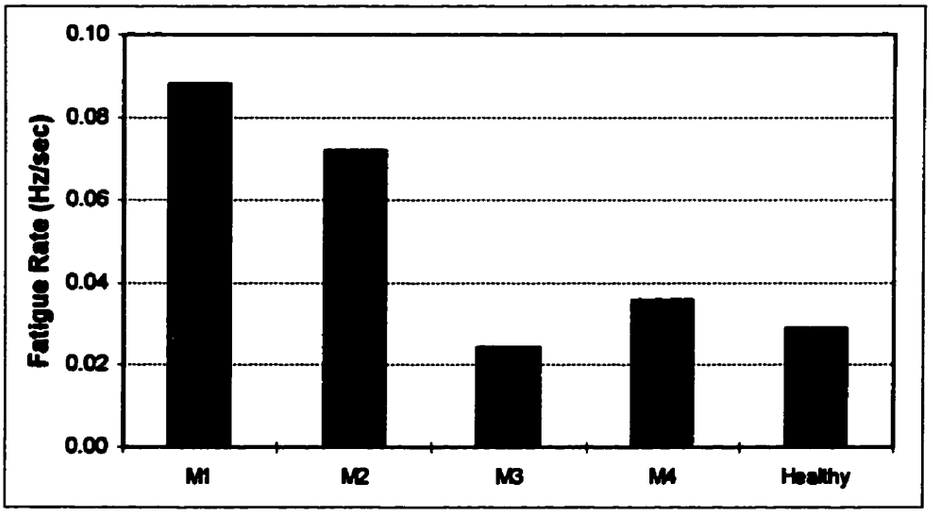

Figure 4.5 The averaged fatigue rate of upper trapezius of healthy subjects and patients in four sessions for experiment B.

4.2.4 Summary of the EMG Results

General results in the Control group:

- The shift of the power spectrum of a prime mover muscle was significantly greater than that of a muscle which was acting as a stabilizer.
- The RMS trend was directly related to the functional role of the involved muscle. It increased almost linearly when the muscle was acting as a stabilizer and was variable when the muscle acted as a prime mover.
- There was a plateau in the MPF trend at the low contraction level. Such a plateau was not observed at the high contraction level.

General results in the Intervention group:

- For position B, the endurance time increased significantly in sessions M3 and M4 compared to that in session M1.
- The fatigue rate of upper trapezius, while it was acting as a prime mover, decreased significantly in sessions M3 and M4 compared to that in session M1.
- The fatigue rate of middle deltoid at the high contraction level decreased significantly in sessions M3 and M4 compared to that in session M1.

Comparison between the Control and the Intervention groups:

- The endurance times of patients were significantly less than those of healthy subjects, especially for the experiment at position B, where the affected muscle (trapezius) acted as the prime mover. This was true even after treatment.
- For patients there was a complete absence of the plateau at the end of MPF trend in muscles of an affected side.
- The fatigue rate of the affected upper trapezius was significantly faster in patients than in healthy subjects.
- The total shift of the mean power frequency of the selected muscles toward lower frequencies was more pronounced in healthy subjects, although it was not statistically significant.
- The RMS value of upper trapezius increased significantly in all healthy subjects while the muscle was acting as a stabilizing synergist; however, its behavior in patients was variable.

4.2.5 Discussion

The EMG Fatigue Pattern of Normal Muscles

That there is a shift of the mean power frequency toward lower frequencies with fatigue is well established in the literature. The trend of a significant shift by the deltoid and a less pronounced shift for the trapezius in an arm abduction or flexion posture has been reported by other researchers [Hansson et al, 1992; Gerdle et al, 1993; Hagberg and Kvarnstrom, 1984]. Studies into the behavior of the RMS have been more anomalous. Gerdle et al [1993] who studied MPF and RMS shifts with fatigue while the upper limb was at 90° shoulder flexion with elbow fully extended, reported a significant increase in RMS for both anterior deltoid and upper trapezius. Stulen and De Luca [1981] reported RMS behavior for deltoid with the EMG signals recorded by both surface electrodes and intramuscular electrodes; their results showed a decrease in RMS for the intramuscular electrode recording and an increase for the surface electrode recording. They explained this contradiction by relating it to the filtering properties of the tissue between the active muscle fibers and the electrodes.

Other researchers have postulated that the synchronization of the active motor units causes the increase of RMS during constant contraction [Person & Mishin, 1964; Lloyd, 1971; Chaffin, 1973]. However, the results of De Luca [1993] do not support such a relationship.

The results of other studies of fatigue in trapezius [Sundelin & Hagberg, 1992; Hansson et al, 1992; Hagberg & Kvarnstrom, 1984] during an abducted or flexed arm posture, showed a significant increase in the trapezius' RMS, while the deltoid's RMS was

either not mentioned or remained constant. The investigators postulated the different behavior was due to the difference in fiber type composition of the two muscles.

While most researchers interpret an increase in RMS as a sign of fatigue, the results of the present study question the use of the RMS parameter as an indicator for fatigue progression. The RMS results of this study showed that there were two distinct patterns for trapezius in the two test positions: one is which there was an almost linear increase while the muscle was acting as a stabilizing synergist (position A) and one in which there was a decrease followed by an increase while the muscle was acting as a prime mover (position B). The latter pattern was also observed for deltoid in position A, in which it acted as a prime mover.

A simpler and perhaps more plausible explanation for the different behaviors of RMS is the functional role of the muscle. In the abducted shoulder position (position A) the middle deltoid is the prime mover muscle, while upper trapezius is a stabilizing synergist muscle. It is therefore most natural that the deltoid should fatigue first. This is borne out by the deltoid's MPF trend (Figure 4.2.a) which is in agreement with previously reported results [Oberg et al, 1992; Gerdle et al, 1993; Hagberg & Kvarnstrom, 1984]. As can be seen from Figures 4.2.a and 4.2.b the MPF shift is significantly more pronounced for deltoid. Since trapezius is considered to be a fatigue-resistant muscle, its less pronounced MPF shift compared to that of middle deltoid is expected. However, the results also show a more pronounced MPF shift for the upper trapezius in position B, during which it is a prime mover, compared to that in position A.

The MPF shift toward lower frequencies can be associated with an increase in RMS values. However, since the firing rate of motor units decreases during fatigue, the RMS value is expected to decrease. These two opposing trends may cancel each other and result in a constant RMS, or, depending on which one is dominant, in an increase or decrease in the RMS behavior. The results of this study show that, in most cases, the RMS of the prime mover muscles (deltoid in position A and trapezius in position B) had a variable pattern of a decrease followed by an increase. But why does this pattern not exist for the RMS of trapezius in position A as it showed a significant linear increase in all trials? The reason can be well explained by the functional role of the involved muscles. The trend of MPF of trapezius does not indicate any significant fatigue, while its RMS increase suggests that either the firing rate or the number of active motor units have increased. Since the external load is constant, the above rationale leads to the conclusion that, as the middle deltoid fatigues, its force output decreases where the upper trapezius muscle accounts for the difference by recruitment of new motor units.

The MPF and RMS trends of the other portions of deltoid and trapezius further support the above reasoning. During the experiments at position A, the RMS values of the anterior and posterior portions of deltoid remained almost constant or increased slightly and their mean MPF shift was 19%. This suggests that the anterior and posterior positions of deltoid in experiment A acted as stabilizers throughout, since abduction cannot be generated by them. Since there would be no reason for these portions of deltoid to recruit new motor units, the effect of increasing the amplitude as a result of MPF decrease, would be canceled out by the decrease in firing rate, hence their constant RMS. As the middle

portion of deltoid fatigued, its contribution to maintaining the external load was shifted to the trapezius, as described before.

The same patterns were observed in the results from the lower portion of trapezius for position B. In this position the RMS values of lower trapezius increased, while there was a slight decrease in the RMS of the upper and middle parts of trapezius; this can be explained by considering that while upper and middle trapezius are prime movers for elevation and retraction, the lower portion acts only as a stabilizing synergist.

The existence of a plateau in the MPF trend at the end of the fatigue process seen only at low contraction level is an interesting phenomenon that brings more insight into muscle behavior. Physiologically the plateau can be explained by:

1- The conduction velocity decreases and itself plateaus at a specific level.

2- There is recruitment of new motor units (probably type-II) in the last stage of fatigue.

The first explanation follows from the direct relationship between MPF and the conduction velocity. However the fact that the MPF data at the high contraction level does not have a plateau and that at this contraction level the final MPF is below that of the final MPF at the low contraction level is evidence against this reasoning as, presumably, at the low contraction level the conduction velocity has not reached its plateau.

The second explanation is the more plausible. As mentioned in Section 2.1, it is believed that type-I fibers are recruited first, particularly by large muscles. As the fibers fatigue, at a low level of contraction, the composition of the active motor unit pool would change to include more type II fibers. These fibers are considered to be fast-twitch fibers and therefore their contraction generates a higher mean power frequency. If new motor

units of type-II are recruited, then their contribution to the overall spectrum will be at the "relatively" higher frequency. This would counteract the effect of the decrease in conduction velocity on the spectrum and results in the plateau. At the high contraction level, it would be expected that all or the majority of both type-I and type-II fibers have already been recruited. Therefore, this balance is not observed.

Also, as was discussed earlier in this section, in most cases the RMS trend of the prime mover muscle during fatigue was associated with a decrease followed by an increase. Incidentally, the starting point of the plateau in the MPF trend and the starting point of the increase in the RMS trend were almost simultaneous (Figure 4.6). This observation supports the theory that new motor units are recruited at the time the plateau occurs.

Implicit support for this second explanation comes from the very recent report by Erfanian et al [1996], who found different stages of MPF and RMS trend during isometric sustained stimulation (increase during potentiation, decrease during fatigue and increase during maximal fatigue).

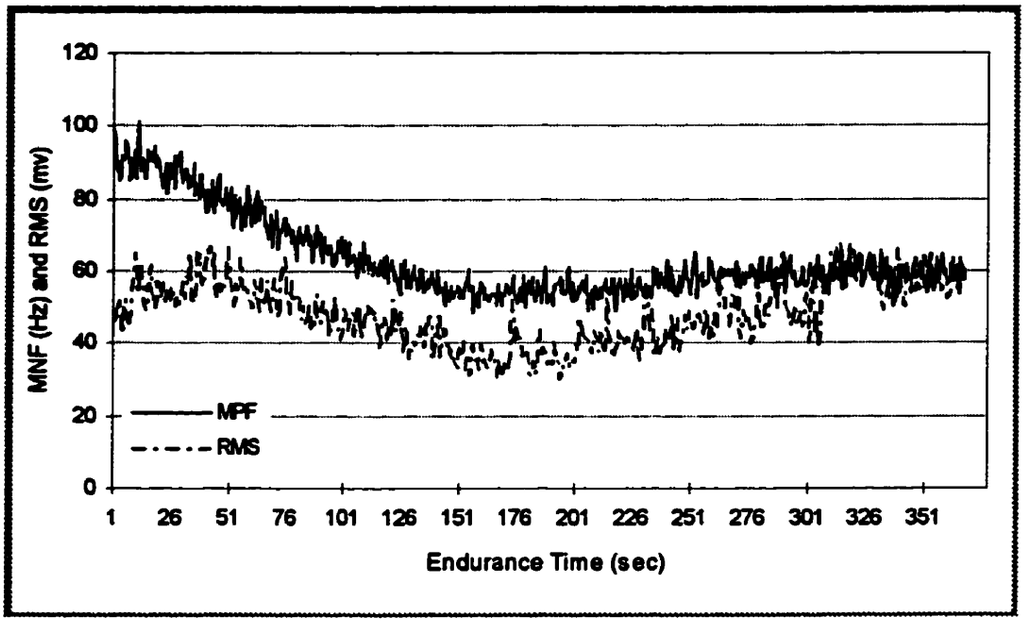

Figure 4.6 MPF and RMS trend of middle deltoid at position A, 0 kg hand load.

EMG Fatigue Patterns of Myalgic Muscles

Based on the results and discussion of the previous part, the major features of the fatigue pattern of healthy muscles can be described as follows: 1- when a muscle acts as a prime mover, its power spectrum has a significant shift toward lower frequencies; 2- when a muscle acts as a stabilizer, its RMS increases almost linearly; 3- when a muscle acts as a prime mover, its RMS is not a good indicator of its fatigue since it does not follow a defined pattern.

These features of the fatigue pattern were different for myalgic muscles. If a stabilizer muscle happened to be myalgic, its RMS did not show a linear increase. The fatigue rate of the myalgic muscles was faster than that seen in the normal muscles. The observation of a faster fatigue rate in myalgic trapezius supports previous findings [Hagberg & Kvarnstrom, 1984; Gogia & Sabbahi, 1994; Oberg et al, 1992].

Interestingly, the total shift of MPF toward lower frequencies for deltoid, which was not an affected muscle, showed a significant difference between healthy subjects and patients, while no difference was seen in its fatigue rate between the two groups. This suggests that fatigue rate is the preferred parameter to show differences between healthy and myalgic muscles.

The difference in the total MPF shift for an unaffected muscle (i.e. deltoid) between healthy subjects and patients might be due to shorter endurance time of the patients. This shorter endurance time is probably the result of pain in the shoulder and neck area, which in turn is due to myofascial trigger points in trapezius.

The complete absence of plateau in the MPF shift of an unaffected muscle (i.e. deltoid) in patients could also be due to the shorter endurance time; the muscle does not contract for a long enough time to reach its maximum limit of fatigue because of the pain in an affected muscle (i.e. trapezius) in the group. All of the patients who participated in this study, except two, had myalgic trapezius bilaterally. For these two patients, the plateau was observed for deltoid on the unaffected side but it was absent in the deltoid of the affected side. This observation suggests strongly that the existence of a myalgic muscle affects the performance of a group of muscles that are in a synergistic or antagonist relationship with that muscle.

The observation of higher initial activity of trapezius in patients compared to that seen in healthy subjects during experiments at position A, may be due to a higher average firing rate in myalgic muscles as reported in Basmajian & De Luca [1985]. However, one may postulate that a myalgic muscle recruits more motor units than a normal muscle for the same contraction level, giving rise to the higher initial activity.

The results of this study showed a significant improvement in EMG fatigue parameters of patients after treatment. Further, the results indicate that the improvement does not appear in the week immediately after treatment but some time later. It must be emphasized that all of the patients except two received several treatments between sessions M1 and M4. However, in all cases the treatment was completed at least two weeks before measurement session M4. The two patients who received only a single treatment had only one or two trigger points in upper trapezius and showed significant improvement at session M2; this improvement was maintained in sessions M3 and M4.

Results also show that, even after treatment, differences remain between a normal muscle and a treated myalgic muscle.

This section has covered the results and discussion of the electrical aspect of this study. The following section presents the results and discussion from the biomechanical aspect.

4.3 Head-Neck Motion Results

The mean head-neck range of motion of five healthy subjects was calculated and compared to the results reported by Ferlic [1962], and Alund and Larsson [1990]. As can be seen from Table 4.2, results from the current method are similar to those previously reported. The slightly higher standard deviation for lateral flexion in this study could be due to the differences in height of our subjects, which would affect the range of motion for lateral flexion and flexion-extension. Test-retest results in healthy subjects yielded correlation coefficients of 0.98 for flexion-extension ($p < 0.001$) and 0.97 for lateral flexion and rotation ($p < 0.004$).

The mean values of head-neck range of motion in patients at different sessions are shown in Table 4.3. Overall it can be seen that there was an increase in range of motion for all movements after treatment was completed. Although only the change in flexion-extension range of motion was statistically significant ($p < 0.0009$), most patients showed some improvement in lateral flexion and rotation. Figure 4.7 shows the flexion-extension range of motion of a patient before and after treatment compared to that of a healthy subject.

Comparison between Tables 4.2 and 4.3 shows that, even after treatment, the range of motion in patients was less than that seen in healthy subjects. This may be due to the fact that the patients were older than the healthy subjects.

A difference in the pattern of motion between healthy individuals and patients was also observed. The patterns of motion for head-neck rotation of one normal subject and one patient are plotted in Figures 4.8.a and 4.8.b. It can be seen that rotation was accompanied by motion in each of the sagittal and frontal planes; this is more pronounced in the patient plot.

Author	Method	# of Subjects	Flexion-Extension	Lateral Flexion	Rotation
Ferlic 1962	Protractor	59	$127^\circ \pm 21.5^\circ$	$74^\circ \pm 14.5^\circ$	$143^\circ \pm 20^\circ$
Alund & Larsson 1990	Electrogoniometer	10	$140^\circ \pm 18^\circ$	$91^\circ \pm 12^\circ$	$153^\circ \pm 16^\circ$
Current study	3-D measurement using video cameras	5	$142^\circ \pm 21^\circ$	$98^\circ \pm 19.5^\circ$	$167^\circ \pm 7^\circ$

Table 4.2 Average head-neck range of motion in normal subjects. All angles are in degrees.

	Flexion-Extension				Lateral Flexion				Rotation			
	M1	M2	M3	M4	M1	M2	M3	M4	M1	M2	M3	M4
M1	-	s	s	s	-	ns	ns	ns	-	ns	ns	ns
M2	-	-	ns	ns	-	-	ns	ns	-	-	ns	ns
M3	-	-	-	ns	-	-	-	ns	-	-	-	ns
Mean	87.7°	101.2°	110°	112°	63.7°	70.9°	68.1°	74.4°	119°	125°	121.9°	129°
STD	26.9°	30.7°	24.9°	22.6°	15°	19.8°	19.6°	20.9°	32.2°	40.9°	40.1°	28.3°

Table 4.3 Significance difference and mean value of head-neck range of motion of patients with myofascial trigger points at different sessions (M1-M4) compared to that of healthy subjects (listed on the last row of Table 4.2). All angles are in degrees. STD = standard deviation. "s" and "ns" refer to statistical significant and non-significant differences between sessions.

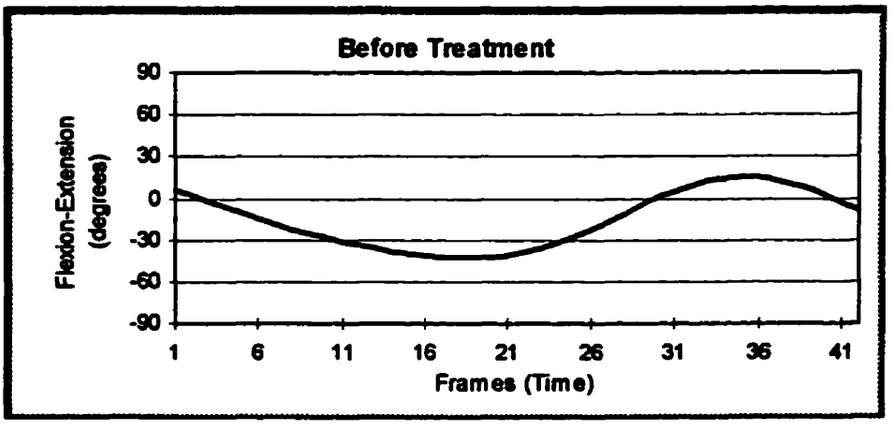

(a)

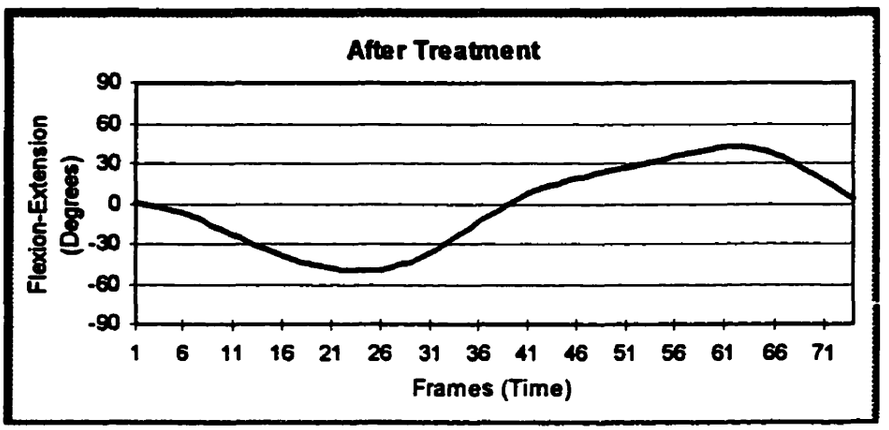

(b)

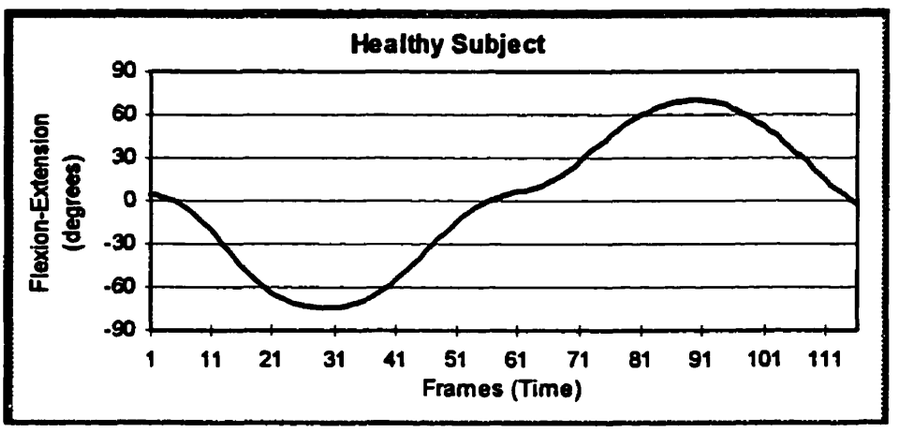

(c)

Figure 4.7 Flexion-extension of a patient before treatment (a), after treatment (b) and a healthy subject (c).

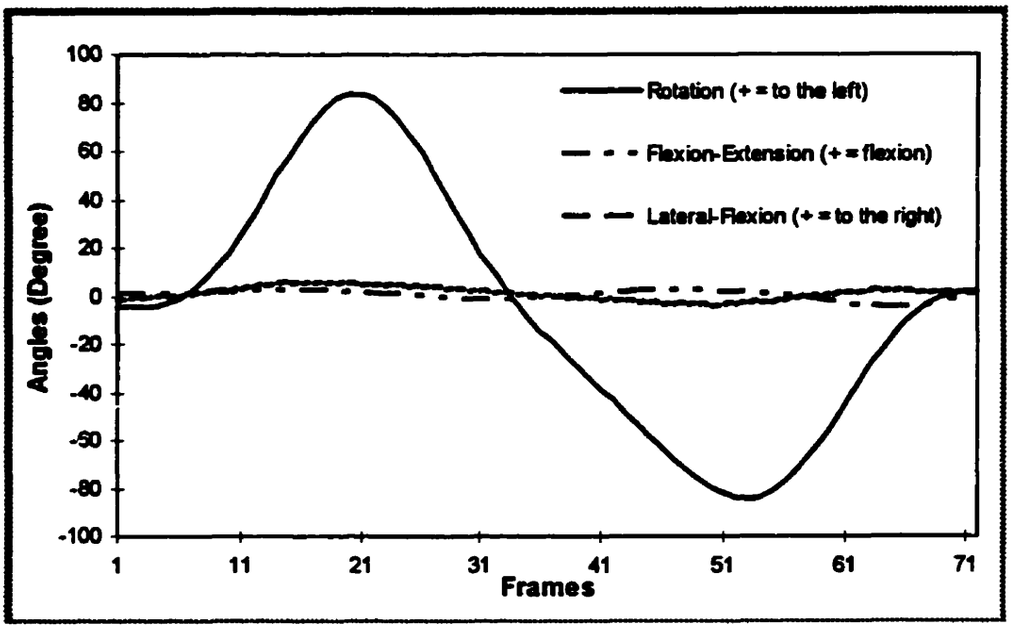

(a)

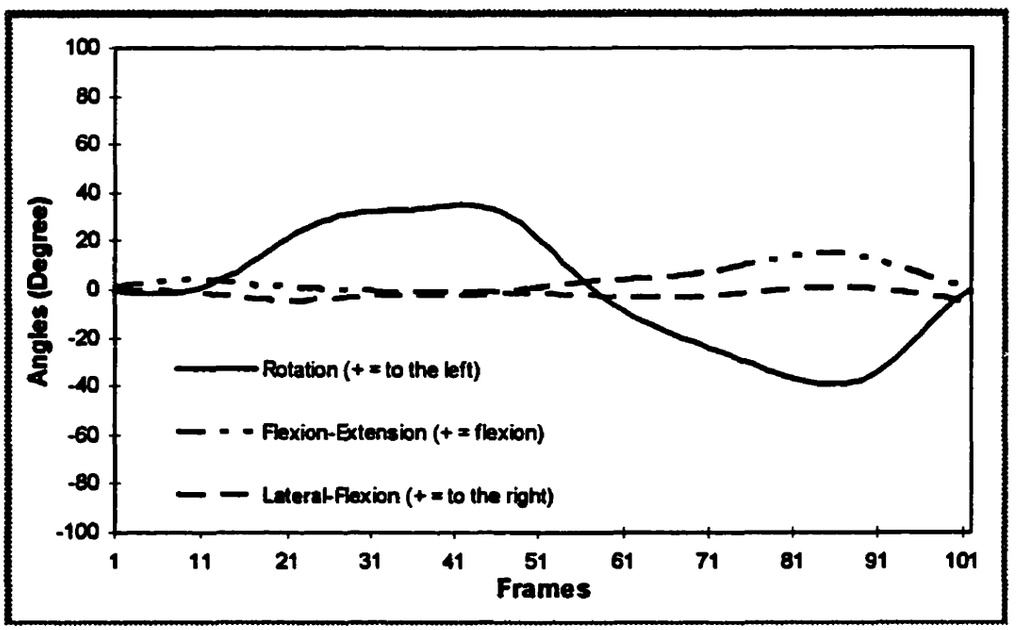

(b)

Figure 4.8 Head-neck rotation of a healthy subject (a) and a patient before treatment (b).

4.3.1 Discussion

The method presented in this thesis showed agreement with previously reported results obtained by different methods for head-neck range of motion of normal subjects. It also showed excellent reproducibility.

Application of the method to measure head-neck range of motion of patients with myofascial trigger points in upper trapezius muscle before and after treatment showed that the head-neck range of motion improved, especially in flexion-extension. The increase in range of motion (typically on the order of 23°) was significant for all patients. Lateral flexion and rotation also increased after treatment in most of the patients, although the change was not statistically significant. It should be noted that treatment was confined to myofascial trigger points in the trapezius and, even after treatment, all patients except the two who did not have trigger points in their other neck muscles, had a limited range of motion.

The pattern of head-neck motion was found to be different between normal subjects and patients, especially during lateral flexion and rotation. Both of these motions were accompanied by greater flexion-extension than that seen in normal subjects. This was expected because it was observed that the patients with a stiff neck usually tried to perform lateral flexion or rotation with the help of extension. This could be due to pain and/or a learned pattern of motion to compensate for the decreased range of motion.

As can be seen the results of biomechanical aspect of this study were consistent with the EMG results. Now, one should look to the subjective results from the patients which is presented in the following section.

4.4 Subjective Measurements

As explained in Section 3.8, besides the EMG and head-neck range of motion data, two subjective measurements were also used: pain and the COPM. This section presents the results of these measurements.

Pain Data- There was no change in pain level of the patients as a result of participating in the experiments of this study; however, there were changes between sessions. The pain level of patients decreased slightly in sessions M2 and M3 and significantly in session M4 compared to that in session M1.

COPM Data- There were significant improvements in the performance and satisfaction level of patients in sessions M3 and M4 compared to those in session M1.

Table 4.4 shows the results of the statistical comparison of pain level and COPM data between sessions as well as their mean values. Figure 4.9 shows the plot of the mean values of pain and the COPM data at different sessions. As can be seen, the pain level is highly correlated with the other parameters, although only its correlation with endurance time was statistically significant ($p < 0.002$). However, it should be noted that since the number of measurement sessions was limited to 4, the lack of statistical significance should be interpreted with caution.

Endurance time was also negatively correlated with fatigue rate. As expected, performance was highly correlated with satisfaction. Figures 4.9 to 4.11 show the mean values of the mentioned parameters at different measurement sessions.

	Pain Score				Performance Score				Satisfaction Score			
	M1	M2	M3	M4	M1	M2	M3	M4	M1	M2	M3	M4
M1	-	ns	ns	s	-	ns	s	s	-	ns	s	s
M2	-	-	ns	ns	-	-	ns	s	-	-	s	s
M3	-	-	-	ns	-	-	-	ns	-	-	-	ns
Mean	4.62	3.56	3.1	1.63	36.5	53.3	53.3	58.3	23.8	32.6	39.9	55.8

Table 4.4 Comparison results of pain and COPM data at sessions M1-M4. "s" and "ns" refer to statistical significant and non-significant differences between sessions.

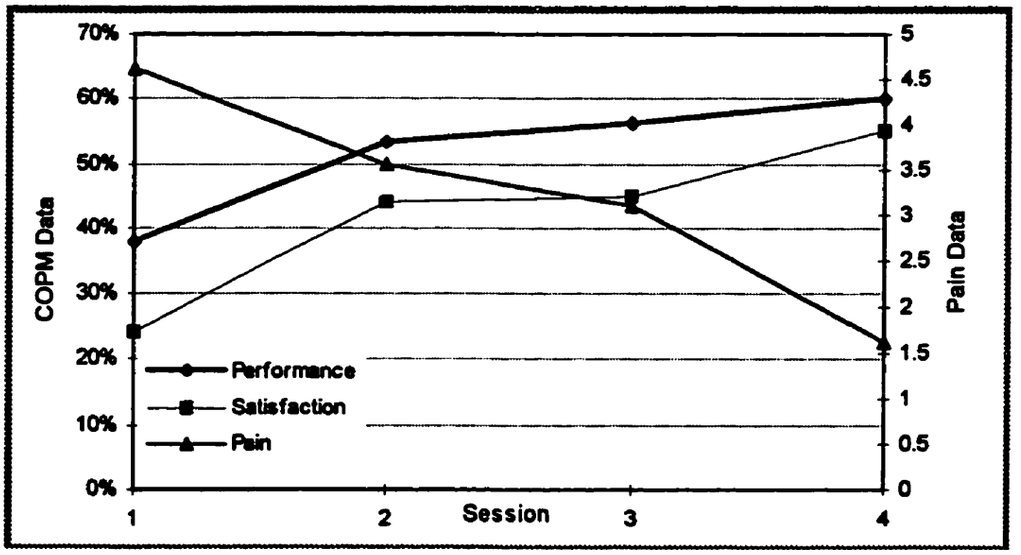

Figure 4.9 Mean values of COPM (Performance and Satisfaction) and pain (VAS) data at different sessions.

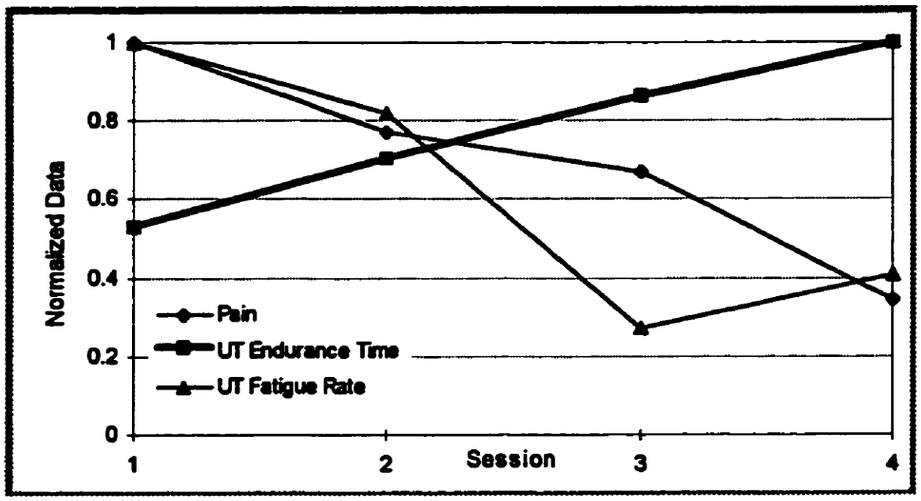

Figure 4.10 Normalized mean values of pain, trapezius' endurance time and fatigue rate at sessions M1-M4.

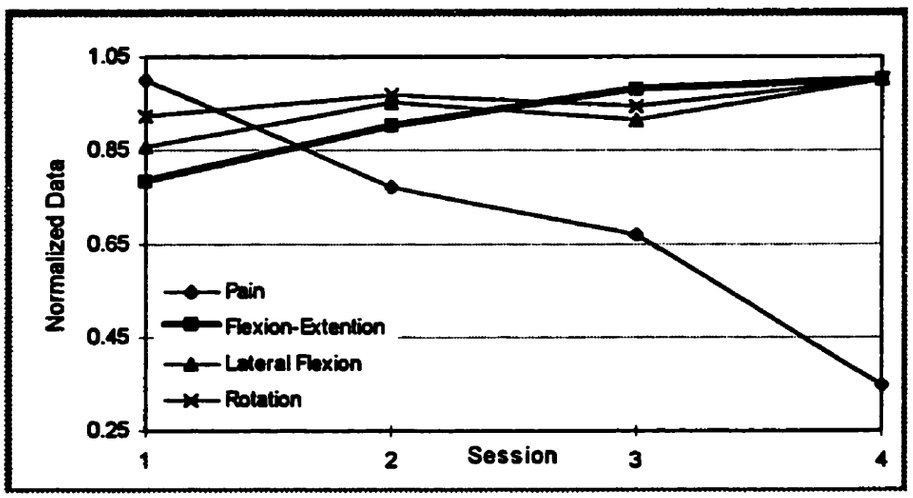

Figure 4.11 Mean values of pain and head-neck range of motion at sessions M1-M4.

4.4.1 Discussion

The subjective data show that patients felt improvement in their daily activities and pain level after a few treatments. Since all patients except two had more than one trigger point in their upper trapezius, their treatment took several sessions to be completed. Patients with fewer trigger points improved immediately after the first treatment. However, for most patients the effect of treatment was apparent only after several treatments. All the subjective results indicate that the effect of treatment was statistically significant in session M4, which occurred at least two weeks after the last treatment.

4.5 Overview

The results of this study challenge the common concept about the fatigue pattern of normal muscles and give rise to a theory about the relationship between the fatigue pattern of a muscle and its functional role as discussed in Section 4.2.1. The fatigue pattern of a normal muscle was compared to the fatigue pattern of myalgic muscles in order to quantify differences and possible changes after treatment.

Overall, the results of objective and subjective measurements indicate a substantial improvement in patients after treatment. Further, the results were consistent and were related to each other. As it can be seen from Figures 4.9 to 4.11, there was a strong relationship between pain, head-neck range of motion, endurance time, fatigue rate and subjective performance and satisfaction of the patients.

While the limitation in head-neck range of motion is directly related to muscle stiffness and pain, these results may indicate that the shorter endurance time and faster

fatigue rate of a myalgic muscle are more likely due to inhibition as a result of pain rather than other possible physiological and/or metabolic changes in the muscle. However, the finding of a significant difference in the RMS behavior of trapezius between the patients and healthy subjects while the muscle was acting as a stabilizing synergist and, during the same experiment finding that the endurance time between the two groups was not significantly different, may indicate a physiological change in the myalgic muscle. Based on this result, one may postulate that there is an inefficiency in motor unit recruitment in a myalgic muscle.

To elaborate further on recruitment inefficiency, the functional role of muscles in a sustained contraction must be considered. As discussed in Section 4.2.1, during a sustained contraction a stabilizer muscle (i.e., trapezius) recruits more motor units to compensate for the reduced force output of the prime mover muscle (i.e. deltoid). The observation of a higher initial RMS in a myalgic trapezius compared to that in a healthy muscle may indicate that the myalgic muscle recruits more motor units than a healthy one at the beginning of contraction. Therefore, one possible explanation is that by the end of the contraction, there are not enough motor units left to be recruited to compensate for the reduced force output of prime mover muscle; hence the variable behavior of myalgic trapezius' RMS and its faster fatigue rate compared to that of a healthy one.

The weakness and fatiguability of muscles associated with myofascial TPs have been related to metabolic changes such as reduced circulation and hypoxia, and/or inhibition of a reflex nature initiated by afferent impulses from an active TP [Basmajian &

De Luca, 1985]. However, to date there is no metabolic evidence to explain the observed higher EMG activity in afflicted muscles compared to that in normal muscles.

CHAPTER 5
CONCLUSIONS AND RECOMMENDATIONS

5.1 Concluding Remarks

The main objective of this study was to investigate the effect of treatment on muscles with myofascial trigger points (TP). Since the muscle most afflicted by this disorder is the trapezius [Travell & Simons, 1983], patients with myofascial trigger points in trapezius were studied before and after treatment and were compared to a control group of healthy individuals who had no history of pain or muscle disorder. To study the effect of treatment, the problem was considered mainly from two viewpoints: electrical and biomechanical. Subjective measurements of patients' performance were also studied.

Electromyography (EMG) was used as a tool to study the electrical aspects of the problem, in particular to compare the fatigue pattern of a myalgic muscle compared to that of a normal muscle. Because the EMG fatigue patterns of normal muscles reported in the literature are inconsistent; therefore, the EMG fatigue pattern of normal muscles was studied in parallel with that of myalgic muscles.

A pilot study during the course of this research showed that the fatigue pattern of a muscle was directly related to its functional role [Moussavi et al., 1996]. As a result, the experiments for the main study were designed in such a way that the fatigue pattern of a muscle could be observed thoroughly. The characteristics of such patterns for normal muscles were defined; the fatigue patterns of myalgic muscles were found to be different.

Further, the EMG fatigue parameters of myalgic muscles were compared before and after treatment. A significant improvement was found after the treatment was completed (Section 4.1.4).

Myofascial trigger points in trapezius are associated with limitation in head-neck motion [Travell & Simons, 1983]. To study the effect of treatment on this motion, a biomechanical model was defined for the head and neck (Section 3.6). A new three-dimensional method was developed to measure head-neck motion (Sections 3.7 and Appendix D). This was used to measure head-neck motion of healthy subjects and of patients before and after treatment. Compared to previously reported head-neck measurements by different methods, the method presented in this thesis yielded reliable results. The results from patients showed a significant improvement in the head-neck range of motion after treatment, which was consistent with the EMG fatigue pattern improvement. The results and the related discussion were presented in Section 4.2.

Lastly, the subjective pain level and perceived disability of patients were measured before and after treatment. These results also showed a significant improvement in the perception of patients about their problem.

Overall, this research has considered the effect of treatment on myofascial trigger points in trapezius muscle from three different aspects as mentioned above. To date, such a thorough study of the effect of treatment for myofascial trigger points has not been described. Although a part of the results challenges some common interpretations of EMG behavior with fatigue, it is believed that these results are pieces of a puzzle that, if put in the right place, would resolve the controversy. Perhaps one of the main contributions of

this research was to find a general picture of EMG behavior with fatigue in both healthy and myalgic muscles that can explain the existing inconsistencies in the literature.

Although this research has tried to consider the problem thoroughly, there were limitations such as:

- having a biased selection of healthy individuals rather than a random selection;
- the lack of available patients who met all inclusion criteria in the original protocol;
- being limited to only using surface electrodes for EMG recording.

Since myofascial trigger points are extremely common in middle aged people, it was very difficult to recruit healthy subjects within the age range of the patient group. Therefore, the mean age of the control group was less than the mean age of patients. Also, finding ten unilaterally affected patients whose deltoid had to be non-affected was impossible during a two year time frame. Further, initially it was hoped that patients would receive treatment only once and therefore their performance three months after treatment could be studied. However, all of the patients except two received treatment several times as they had more than one trigger point. Therefore, only measurement session M4 can be considered as the "time after treatment".

5.2 Recommendations for Future work

Although the results of this research were consistent, more investigation with larger numbers of patients is required to research the long-term effect of treatment for myofascial trigger points. Surface electrode EMG recording represents only the gross electrical activity of the muscle; intramuscular EMG recording and some molecular

biological studies are required to investigate the accuracy of the theories presented in Chapter 4. This research was limited to the use of surface electrodes for ethical and logistical reasons. With intramuscular EMG recording, it would be exciting to study the possible relationship of the EMG parameters to the reported fiber type composition of the muscle.

The function related fatigue pattern of muscles presented in this thesis questions the common interpretation of the RMS behavior during muscle fatigue. More experiments, in which the functional role of the involved muscle is known, need to be designed to verify the theory.

Lastly, the head-neck measurement method should be combined with the methods for measuring clavicular motion presented in [Moussavi et al, 1996] and shoulder motion presented in [Safaee-Rad et al., 1990] to provide a complete upper body model and motion measurement system.

APPENDIX A

Power Spectrum Estimation

Suppose $x(t)$, $-T/2 \le t \le T/2$, is one of the many possible ensemble members of a stochastic process $X(t)$. Then the power spectrum $\hat{S}_{xx}(f)$, may be calculated as follows:

$$\begin{aligned}\hat{S}_{xx}(f) &= \frac{1}{T}\left|\int_{-T/2}^{T/2} x(t)e^{-j2\pi ft}dt\right|^2 \\ &= \frac{1}{T}\int_{-T/2}^{T/2} x(t)e^{-j2\pi ft}dt \int_{-T/2}^{T/2} x(t')e^{j2\pi ft'}dt'\end{aligned}$$

Let $u = t - t'$, and $v = t' = t - u$. If $u > 0$, its range is $[0, T]$, hence v has the range $[-T/2, T/2 - u]$. If $u < 0$, its range is in $[-T, 0]$, and v has the range $[-T/2 - u, T/2]$. Therefore, the above equation can be written as the following:

$$\begin{aligned}\hat{S}_{xx}(f) &= \frac{1}{T}\int_0^T \int_{-T/2}^{T/2-u} x(v)x(u+v)e^{-j2\pi fu}dvdu + \frac{1}{T}\int_{-T}^{0} \int_{-T/2-u}^{T/2} x(v)x(u+v)e^{-j2\pi fu}dvdu \\ &= \int_{-T}^{T} \hat{c}_{xx}(u)e^{-j2\pi fu}du \qquad -\infty < f < \infty,\end{aligned} \tag{A.1}$$

where $\hat{c}_{xx}(u)$ is an estimate of the sample autocorrelation of $x(t)$ defined as

$$\hat{c}_{xx}(u) \equiv \frac{1}{T}\int_0^{T-|u|} x(t)x(t+u)dt, \qquad 0 \le |u| \le T.$$

The expected value of $\hat{c}_{xx}(u)$ is

$$E[\hat{c}_{xx}(u)] = \frac{1}{T}\int_0^{T-|u|} E[x(t)x(t+u)]dt = \frac{1}{T}\int_0^{T-|u|} c_{xx}(u)dt = \begin{cases} c_{xx}(u)\left[1 - \dfrac{|u|}{T}\right] & 0 \le u \le T \\ 0 & |u| > T \end{cases}$$

$$\Rightarrow E[\hat{S}_{xx}(f)] = \int_{-T}^{T} E[\hat{c}_{xx}(u)]e^{-j2\pi fu}du = \int_{-T}^{T} c_{xx}(u)\left[1-\frac{|u|}{T}\right]e^{-j2\pi fu}du$$

or using the convolution theorem:

$$E[\hat{S}_{xx}(f)] = S_{xx}(f) * T\left(\frac{\sin \pi fT}{\pi fT}\right)^2, \qquad \text{(A.2)}$$

where * denote the convolution operator and $S_{xx}(f)$ is the Fourier transform of $c_{xx}(u)$, the true sample spectrum. Therefore, $\hat{S}_{xx}(f)$ may be considered to be an asymptotically unbiased estimator for the power spectrum of the random process $X(t)$.

$$\therefore \lim_{T\to\infty} E\left[\hat{S}_{xx}(f)\right] = \int_{-\infty}^{\infty} c_{xx}(u)e^{-2\pi fu}du = S_{xx}(f)$$

However, as derived in [Papoulis, 1977], the variance of $\hat{S}_{xx}(f)$ is not small. In fact for any T, $\text{var}[\hat{S}_{xx}(f)] \geq E^2[\hat{S}_{xx}(f)]$, which implies $\hat{S}_{xx}(f)$ is not a good estimator.

To reduce the variance of the estimator, a lag window may be used for the sample autocorrelation $\hat{c}_{xx}(u)$. Therefore the spectrum estimator may be defined as

$$\hat{S}_w(f) = \int_{-T}^{T} \hat{c}_{xx}(u)w(u)e^{-j2\pi fu}du = \hat{S}_{xx}(f) * W(f),$$

where *w(u)* is a lag window, which takes significant values only in an interval *(-M, M)* such that $M < T$. Then, one has

$$E[\hat{S}_w(f)] = E[\hat{S}_{xx}(f)] * W(f) = S_{xx}(f) * T\left(\frac{\sin \pi fT}{\pi fT}\right)^2 * W(f). \qquad \text{(A.3)}$$

To have a reliable estimation, the duration of *W(f)* must be large compared to *1/T*. The variance of $\hat{S}_w(f)$ is given by Jenkins and Watts [1968]

$$\text{var}[\hat{S}_w(f)] \approx \frac{1}{T} S^2_{xx}(f) E_w, \tag{A.4}$$

where E_w is the energy of window and is defined as

$$E_w = \int w^2(u) = \int_{-\infty}^{\infty} W^2(f) df .$$

To satisfy the small variance requirement, as has been showed by Papoulis [1977], one must choose the length of window such that $E_w \leq 2M$, $M << T$, and also *w(u)* must take significant values near the origin only. On the other hand, smoothing the spectrum increases the bias and as usual, one needs to compromise between bias and variance. However, if the spectrum is constant enough over the range of *(-1/M, 1/M)*, which is the distance between the first zeros on either side of the Fourier transform of the lag window, then

$$E[\hat{S}_w(f)] \approx \hat{S}_{xx}(f) \int_{-\infty}^{\infty} W(f) df = \hat{S}_{xx}(f) w(0) = \hat{S}_{xx}(f) \text{ for } w(0) = 1$$

Therefore, there is no extra bias other than the inherent bias, with the method of smoothing even though the lag window has been made short to reduce the variance [Jenkins & Watts, 1968].

To reduce the inherent bias of the spectrum estimator, which is a result of limiting the signal to the period *(-T/2, T/2)*, another window, called data window, may be used for the data samples such that $x_c(t) = x(t)c(t)$, where $c(t) = 0$ for $t > T/2$. Then, the spectrum estimator is defined as

$$\hat{S}_c(f) = \frac{1}{T} \left| \int_{-T/2}^{T/2} x_c(t) e^{-j2\pi ft} dt \right|^2 . \tag{A.5}$$

According to Papoulis [1977], the best data window, which provides the minimum bias, is the optimum energy window and is defined as

$$c(t) = \cos(\frac{\pi t}{T}), \qquad |t| \le T/2.$$

Then, to reduce the variance of $\hat{S}_c(f)$, a spectral window is convolved with $\hat{S}_c(f)$:

$$\hat{S}_{cw}(f) = \hat{S}_c(f) * W(f),$$

where $W(f)$, is a spectral window with requirements explained earlier in this section. To minimize the bias, $c(t)$ must be chosen such that

$$\int_{-T}^{T} c^2(t)dt = \int_{-\infty}^{\infty} C^2(f)df = 1.$$

If T is sufficiently large, then $\hat{S}_c(f)$ is an unbiased estimator and the bias of $\hat{S}_{cw}(f)$ is due to smoothing only [Papoulis, 1977].

Three examples of windows are the Bartlett, Rectangle, and Hamming windows:

$$w_{Bartlett}(u) = \begin{cases} 1 - \frac{|u|}{M} & |u| \le M \\ 0 & |u| > M \end{cases},$$

$$w_{Rect}(u) = \begin{cases} 1 & |u| \le M \\ 0 & |u| > M \end{cases},$$

$$w_{Hamming}(u) = \begin{cases} 0.54 - 0.46\cos(\frac{\pi}{M}(u+M)), & |u| \le M \\ 0, & |u| < M \end{cases}.$$

By using the above windows as spectral windows the variance of the spectrum estimate for each of the windows can be determined from Equation (A.4):

$$Var_{Hamming}[\hat{S}_{xx}(f)] \approx 0.3974 M \frac{s_{xx}^2(f)}{T},$$

$$Var_{Bartlet}[\hat{S}_{xx}(f)] \approx \frac{2}{3} M \frac{s_{xx}^2(f)}{T},$$

$$Var_{Rectangel}[\hat{S}_{xx}(f)] \approx 2M \frac{s_{xx}^2(f)}{T}.$$

APPENDIX B

Estimation of Mean and Median Frequencies

Let $S(f)$ be the power spectrum of a random process, $x(t)$. Then its median and mean frequencies are defined as

$$\int_0^{f_{med}} S(f)df = \frac{1}{2}\int_0^{\infty} S(f)df \tag{B.1}$$

$$f_{mean} = \frac{\int_0^{\infty} fS(f)df}{\int_0^{\infty} S(f)df}. \tag{B.2}$$

Since $x(t)$ is a realization of a random process in $-T/2 \le t \le T/2$, then, $\hat{S}(f) = \frac{1}{T}\left|\int_{-T/2}^{T/2} x(t)e^{-j2\pi ft}\right|^2$ is also regarded as a realization of a random process, which is the power spectrum of the random signal. Therefore, we can only estimate the median frequency from $\hat{S}(f)$ and therefore it is a random variable. The same argument is true for f_{mean}.

Finding the random characteristics of the mean frequency is more straight forward than those of the median frequency. Assuming that the estimate of the spectrum is normalized: $\int_0^{\infty} \hat{S}(f)df = 1$ it follows from Equation B.2 that:

$$E[\hat{f}_{mean}] = E\left[\int_0^{\infty} f.\hat{S}_{xx}(f)df\right] = \int_0^{\infty} f.E[\hat{S}_{xx}(f)]df = \int_0^{\infty} f\int_{-T}^{T} c_{xx}(u)\left[1-\frac{|u|}{T}\right]e^{j2\pi fu}du$$

If $T \to \infty$, then $E\left[\hat{f}_{mean}\right] \to f_{mean}$, which implies it is an asymptotically unbiased estimator.

For the median frequency estimation, the following proof shows that it is convergent in a probability sense.

Proof of Convergence

Let $\int_0^{\infty} \hat{S}(f)df = 1$ and that $\hat{S}(f) \geq 0 \ \ \forall f$. In this case, the spectrum looks like a probability density function, with a cumulative distribution function defined as $\hat{F}_x(\hat{f}) = \int_0^{\hat{f}} \hat{S}(f)df$, which is the probability of the event $\{x \leq \hat{f}\}$. Similarly define $F_x(f) = \int_0^{f} S(f)df$ as the cumulative distribution function of the true spectrum. To prove that the median frequency estimator is convergent in a probability sense, one must prove that $\Pr\left\{\left|\hat{f}_{med_n} - f_{med}\right| > \varepsilon\right\} \to 0$, for any given $\varepsilon > 0$ and for any observation time. For simplicity the notation of $\hat{F}$ and F is used to refer to $\hat{F}_x(\hat{f})$ and $F_x(f)$, respectively. For a normalized spectrum

$$\int_0^{\hat{f}_{med}} \hat{S}(f)df = 1/2 \Rightarrow \hat{f}_{med} = \hat{F}^{-1}(1/2)$$

$$\int_0^{f_{med}} S(f)df = 1/2 \Rightarrow f_{med} = F^{-1}(1/2).$$

Then

$$\begin{aligned}\Pr\left\{\left|\hat{f}_{med}-f_{med}\right|>\varepsilon\right\} &= \Pr\left\{\hat{f}_{med}>f_{med}+\varepsilon \text{ or } \hat{f}_{med}<f_{med}-\varepsilon\right\} \\ &\le \Pr\left\{\hat{f}_{med}>f_{med}+\varepsilon\right\}+\Pr\left\{\hat{f}_{med}<f_{med}-\varepsilon\right\}\end{aligned} \quad \text{(B.3)}$$

Since the cumulative distribution function of the spectral density, (either $\hat{F}$ or F), is a monotonic increasing function, Equation B.3 can be written as

$$\begin{aligned}\Pr\left\{\hat{f}_{med}>f_{med}+\varepsilon\right\} &= \Pr\left\{\hat{F}(\hat{f}_{med})>\hat{F}(f_{med}+\varepsilon)\right\} \\ &= \Pr\left\{1/2>\hat{F}(f_{med}+\varepsilon)\right\}\end{aligned}$$

Similarly,

$$\begin{aligned}\Pr\left\{\hat{f}_{med}<f_{med}-\varepsilon\right\} &= \Pr\left\{\hat{F}(\hat{f}_{med})<\hat{F}(f_{med}-\varepsilon)\right\} \\ &= \Pr\left\{1/2<\hat{F}(f_{med}-\varepsilon)\right\}\end{aligned}$$

Therefore,

$$\Pr\left\{\left|\hat{f}_{med}-f_{med}\right|>\varepsilon\right\} \le \Pr\left\{\hat{F}(f_{med}+\varepsilon)<1/2\right\}+\Pr\left\{\hat{F}(f_{med}-\varepsilon)>1/2\right\}. \quad \text{(B.4)}$$

If one shows that each term of the above inequality tends to zero, then the proof is complete. For the first term of the right side of the above inequality write:

$$\begin{aligned}\Pr\left\{\hat{F}(f_{med}+\varepsilon)<1/2\right\} &= \Pr\left\{\hat{F}(f_{med}+\varepsilon)-F(f_{med}+\varepsilon)<1/2-F(f_{med}+\varepsilon)\right\} \\ &= \Pr\left\{F(f_{med}+\varepsilon)-\hat{F}(f_{med}+\varepsilon)>F(f_{med}+\varepsilon)-1/2\right\} \quad \text{(B.5)} \\ &= 1-\Pr\left\{F(f_{med}+\varepsilon)-\hat{F}(f_{med}+\varepsilon)\le\delta\right\}\end{aligned}$$

where $\delta = F(f_{med}+\varepsilon)-1/2$. Since $\varepsilon>0$, and the distribution function of the spectrum is monotonically increasing, then $F(f_{med}+\varepsilon)>F(f_{med})$. Therefore, δ is positive. But for a positive ,

$$\Pr\left\{F(f_{med}+\varepsilon)-\hat{F}(f_{med}+\varepsilon)\le\delta\right\}\to 1 \text{ as } \hat{F}\to F,$$

and therefore, the probability of the left side of Equation B.5 tends to zero. In the same manner the second term of the inequality B.4 yields:

$$\Pr\left\{\hat{F}(f_{med} - \varepsilon) > 1/2\right\} \to 0 \text{ as } \hat{F} \to F.$$

Therefore, $\Pr\left\{\left|\hat{f}_{med} - f_{med}\right| > \varepsilon\right\} \to 0$ and the proof is complete. The goodness of median and mean frequency estimation is completely dependent on the goodness of the estimation of the spectrum of the signal. If one has a reliable estimation of spectrum, then the reliability of the median and mean frequency estimators follow.

Appendix C

A Solution to Redundancy of Euler Angles in Human Motion Measurement

Anatomical angles associated with human movement are of interest in many fields. Although goniometers, which measure anatomical angles directly, have been used, they are inaccurate and are not easily applied to all body joints. A common procedure to measure human motion, is to define a model, place external markers on the surface of the limbs or on the bones, define a model, capture the motion on video tape, digitize the coordinates, and then calculate the relative angles between joints [Kennedy et al., 1989]. The theory of Euler angles has been applied to calculate the anatomical angles in elbow motion [Chao et al., 1980], in the spine [Brown et al., 1976], and in upper limb movement [Langrana, 1981; Safaee-Rad et al., 1990].

An inherent problem with most anatomical angle calculation is the redundancy of the system, i.e., for each position of markers there are at least two different sets of angles for joints having more than one degree of freedom (DOF). This problem has either been simply ignored or addressed inadequately [Langrana, 1981]. It is important to note that for two dimensional measurement such as gait studies, the redundancy problem does not exist. Further, if the calculation is limited to measuring only the angle between two body segments then, because this is also in essence a two-dimensional approach, redundancy is not a factor. The problem of solving for Euler angles is that there is not a unique solution to the set of non-linear equations of 3.5. Langrana [1981] addressed this prcblem and tried

to obtain a unique solution by using the arctangents from Equation 3.2. Beside the fact that his method was undefined at $\theta = 90^{o}$, the system is still redundant. Most human motion measurement is typically done by video taping [Chow, 1993; Safaee-Rad et al., 1990; Whittle, 1982]. Since the motion in successive video frames does not change substantially, the non-uniqueness of the solution can be overcome by simply keeping track of the previous angles.

Proposed Algorithm

Assume that initially the angles are determined by choosing the following equations from matrix T (Equations 3.2 and 3.6) and to solve for the principal value of each angle (the principal value is defined as the value of the angle in the first or fourth quarter of a trigonometric circle):

$$\theta_{est} = \sin^{-1}(\vec{y}_2.\vec{z}_1),$$

$$\varphi_{est} = \cos^{-1}\left(\frac{\vec{y}_2.\vec{y}_1}{\cos\theta_{est}}\right),$$

$$\psi_{est} = \cos^{-1}\left(\frac{\vec{z}_2.\vec{z}_1}{\cos\theta_{est}}\right).$$

Define $t_{21} = -\sin\varphi\cos\theta$, $t_{13} = -\cos\theta\sin\psi$, $p\theta$ = previous θ (from previous frame), and $p\varphi$ = previous φ (again from the previous frame). Then the procedure for calculating the correct angles is as follows:

1. Check if θ has a considerable difference (i.e., more than a threshold defined by the user) compared to the previous frame. A considerable difference indicates that the first calculation of θ_{xz} is not correct. In this case go to step 2, otherwise go to step 3.
2. Choose θ to be in the second or third quarter if θ_{xz} is positive or negative, respectively. Recalculate φ_{xz}, ψ_{xz}, t_{21} and t_{13}, then go to step 3.
3. Check if t_{21} is equal to T_{21}. (φ_{xz} has been estimated through its cosine value, therefore it must be checked by an equation of matrix T, which involves its sin value.) If the answer is "No", change φ to $-\varphi_{xz}$, then go to step 4. Otherwise, directly go to step 4.
4. Check angle φ with $p\varphi$. If the difference is less than the threshold, go to step 5. Otherwise, go back to the step 2, change θ, recalculate φ_{xz}, ψ_{xz}, t_{21}, t_{13} and repeat steps 3 and 4. This time the result of the step 4 is "Yes". Go to step 5.
5. Check the value of the ψ angle by checking t_{13} with T_{13}. If $t_{13} = T_{13}$ go directly to the next step. Otherwise, change ψ angle to $-\psi_{xz}$ and then proceed to the next step.
6. Store the three angles, update the previous angles, and return to the step 1 to process the next frame.

A flowchart of the above procedure is shown in Figure C.1.

The proposed algorithm can be applied to any model which uses Euler angles for calculating anatomical angles. The principal idea of the algorithm is to keep track of two angles for the joints which have a wide range of motion, such as θ and φ of a 3 DOF joint. The reason for tracking two angles is as follows: assume that only the θ angle is tracked. If the previous θ is very close to $\pm 90^{\circ}$, then even if the difference between θ_{xz} and the previous θ is less than the threshold, θ_{xz} may be incorrect. There are two methods to

overcome this problem. One is to keep track of another angle such as φ (as described), the other is to check if the previous θ is in the range of $90^{\circ} \pm threshold$. In the second method, the choice of threshold is crucial and the accuracy of the algorithm is dependent on the threshold value, hence on the camera frame rate and on the sampling rate for digitization. A threshold of 10° was found to be satisfactory for determination of upper limb and head-neck motion during activities of daily living. In the first approach, the choice of threshold is not critical because, even if the algorithm fails at the first step, the incorrect θ causes a large change in φ, and therefore it will be corrected when φ is compared with previous φ. Therefore, the first method is more reliable. As long as the difference of the angles between two frames being processed is less than 90°, the proposed algorithm gives the correct results. A large difference (close to 90°) of the same angle in two digitized frames, though not impossible is, however, very unlikely and essentially implies that the sampling rate was chosen improperly for the studied motion. The proposed algorithm's ability to resolve the redundancy problem was tested and verified on extensive data both from simulation and from human upper limb motion and head-neck motion.

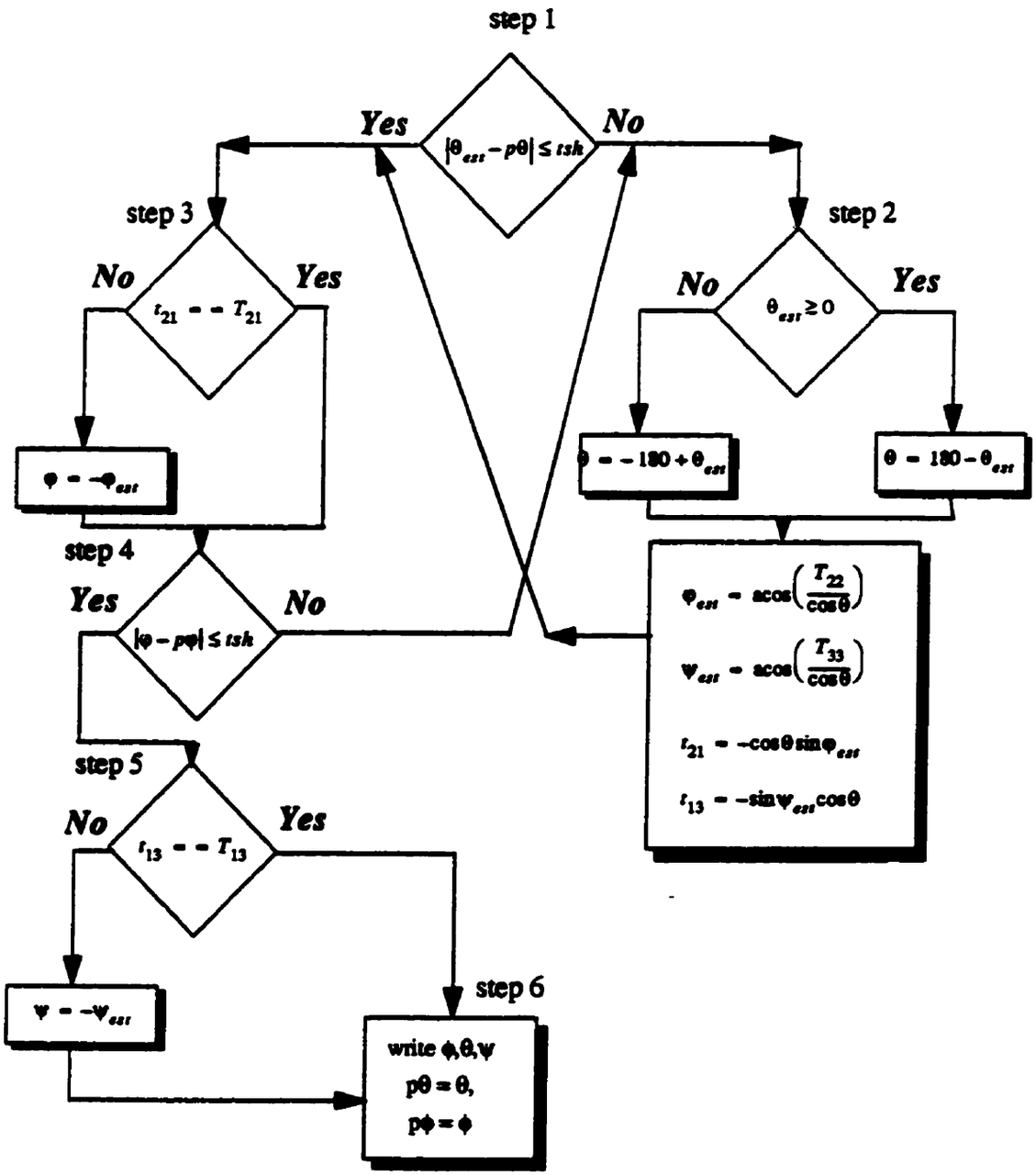
step 1
Yes
$|\theta_{est} - p\theta| \le tsh$
No
step 3
step 2
No
$t_{21} = -T_{21}$
Yes
No
$\theta_{est} \ge 0$
Yes
$\varphi = -\varphi_{est}$
$\theta = -180 + \theta_{est}$
$\theta = 180 - \theta_{est}$
step 4
Yes
$|\varphi - p\varphi| \le tsh$
No
$\varphi_{est} = \arccos\left(\frac{T_{22}}{\cos\theta}\right)$
$\psi_{est} = \arccos\left(\frac{T_{33}}{\cos\theta}\right)$
$t_{21} = -\cos\theta\sin\varphi_{est}$
$t_{13} = -\sin\psi_{est}\cos\theta$
step 5
No
$t_{13} = -T_{13}$
Yes
step 6
$\psi = -\psi_{est}$
write ϕ,θ,ψ
$p\theta = \theta$,
$p\phi = \phi$

Figure C.1

APPENDIX D

Euler Angle Calculation Program

A window based program has been written with MATLAB software. The program allows the user to choose the input file from any directory and writes the name of output files in the output window as shown in Figure D.1. A threshold can be chosen by user or the default threshold (10) is used. The program is able to recognize the missing markers and also misdigitization. In each case it prints appropriate messages in the message window and waits for the user's command. For example, if there is some missing markers it skips the frame and lets the user know the number of the skipped frame. If there is some misdigitization, the program asks the user to ignore or to estimate the location of marker by linear interpolation and continues. There is also a help window which explains the procedure to run the program. This program has been written in two versions: one for head-neck motion and another for upper limb motion. The marker placement is important; for head-neck motion the marker placement is the same as explained in Section 3.7 and for upper limb motion the marker placements are only described in its help window (unpublished work). The output files are both the raw and filtered calculated angles for each motion. The angles for each motion are also plotted on the screen.

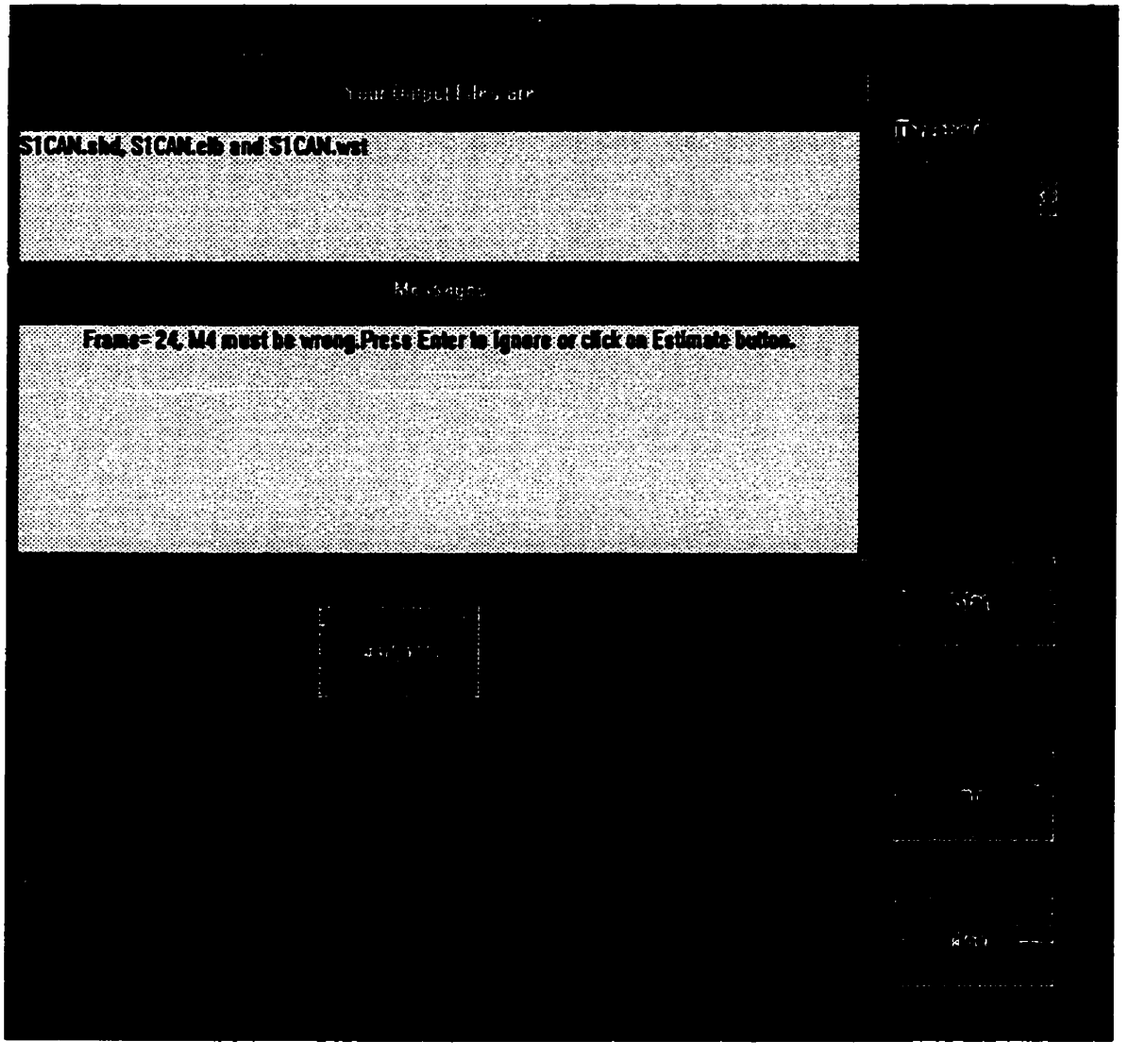

Figure D.1 The Euler angle calulation program.

Chaffin D. B., Localized muscle fatigue: definition and measurement, *J. Occup. Med.*, 15:346-354, 1973.

Chao E.Y., An K.N., Morrey B.F. and Askew L.J., Electrogoniometer for the measurement of human elbow rotation. *J. Biomedical Eng.*, 102: 301-310, 1980.

Chao E., Tanaka S., Korinek S. and Cahalan T., Measurement of neck range and pattern of movement. *J. of Biomechanics.*, 22 (10):996, 1989.

Chow J.W., A panning videographic technique to obtain selected kinematic characteristics of the strides in sprint hurdling. *J. Appl Biomed.*, 9: 149-59, 1993.

Cleveland D., Diagrams for showing limitation of movements through joints. *J. Can. Med. Assoc.*, 8:1070-1076, 1918.

De Luca C.J., Synchronization of motor unit firing in several human muscles. *J. Neurophysiology*, 70(5): 2010-2023, Nov. 1993.

Durette M. R., Rodriquez A., Agre J. C. and Silverman J. L., Needle electromyographic evaluation of patients with myofascial or fibromyalgic pain. *Am. J. Phys. Med. Rehab.*, 70(3):154-156, June 1991.

Enoka R. M., *Neuromechanical basis of Kinesiology, 2nd ed.*, Human Kinetics, Windsor, ON, 1988.

Erfanian A., Chizeck H. and Hashemi R., Excitation-contraction fatigue during sustained electrical stimulation of paralyzed muscle, *Proc. IEEE EMB Conf.*, 782, 1996.

Ferlic D, Range of motion of "normal" cervical spine. *Bull Johns Hopkins Hosp.*, (110):59-65, 1962.

Fielding J. Cineroentgenography of normal cervical spine. *J. Bone Joint Surg [Am]*, 39:1280-1288, 1957.

Fisk G. H. and Colwell G., Shoulder movements in health and disease, *Arch. Phys. Med. Rehab.*, 35: 149-155, 1954.

Freund H., Dietz V., Wita C. W. and Kapp H., Discharge characteristics of single motor units in normal subjects and patients with supraspinal motor disturbances, *New Dev Electromyography Clin. Neurophysiol.*, 3:242-250, 1973.

Fricton J. and Awad E., Myofascial pain and fibromyalgia, *Advances in pain research and therapy*, 17, New York, Raven Press., 1990.

Fricton J. R., Auvinen M. D., Dykstra D. and Schiffman E., Myofascial pain syndrome: Electromyographic changes associated with local twitch response. *Arch. Phys. Med. Rehab.*, 66:314-316, May 1985.

Gerdle B., Edstrom M. and Rahm M., Fatigue in the shoulder muscles during static work at two different torque levels. *Clinical Physiology*, 13:469-482, 1993.

Gielen, C. and Denier Van Der Gon J. , The activation of motor units in coordinated arm movements in humans, *News in Physiological Sciences*, 5:159-163, 1990.

Gogia P. and Sabbahi M., Electromyographic analysis of neck muscle fatigue in patients with osteoarthritis of the cervical spine, *Spine*, vol. 19 no. 5, pp. 502-506, 1994.

Gray's Anatomy, 13th edition, Clemente, C. D. (ed.), Lea & Febiger, Philadelphia, Pa., 1985.

Guyton A.C., *Textbook of Medical Physiology*. W.B. Sauders Company, Philadelphia, Pa., 4th edition, 1971.

Hagberg M. and Kvarnstrom S., Muscular endurance and electromyographic fatigue in myofascial shoulder pain. *Achive of Physical Medicine Rehabilitation*, 65:522-525, Sept. 1984.

Hamlyn P. F., Peggington J., Soo K C., "The cervical plexus and the motor supply to the trapezius [Abstract]", *Scientific Program British Association of Clinical Anatomists Annual Meeting*, June 1986.

Hansson G., Stromberg U., Larsson B., et al., Electromyographic fatigue in neck/shoulder muscles and endurance in women with repetitive work, *Ergonomics*, 35(11): 1341-1352, 1992.

Hary D., Belman M. J., Propst J. and Lewis S., A staistical analysis of the spectral moments used in EMG test of endurance, *J. Appl. Physiol.*, 53:779-783, 1982.

Hassard T. H., *Understanding Biostatistics*. St. Louis: Mosby Year Book, 1991.

Hubbard D. R. and Berkoff G. M., Myofascial trigger points show spontaneous needle EMG activity. *Spine*, 18(13)1803-1807, 1993.

Huskisson E. C., Measurement of pain, *Lancet*, 9:1127-1131, Nov. 1974.

Inman V. T., Saunders F. and Abbott L. C., Observations on the function of the shoulder joint, *J. Bone & Joint Surgery*, XXVI(1):1-29, Jan. 1944.

Larsson S. E., Bengtsson A., Bodegard L., et al., Muscle changes in work-related chronic myalgia, *Acta. Orthop. Scand.*, 59(5): 552-556, 1988.

Lindman R., Eriksson A. and Thornell L. E., Fiber type composition of the human male trapezius muscle: enzyme-histochemical characteristics, *American J. Anatomy*, 189: 236-244, 1990.

Lindstrom L., Magnusson R. and Petersen I., Muscular fatigue and action potential conduction velocity changes studied with frequency analysis of EMG signals. *Electromyograpy*, 4:341-353, 1970.

Lloyd A. J., Surface electromyography during sustained isometric contractions, *J. Appl. Physiol.*, 30:713-719, 1971.

McBroom P., Walsh N. E. and Dumitru D., Electromyography in primary fibromyalgia syndrome. *The Clinical J. of Pain*, 4(2):117-119, 1988.

McComas A. J., *Skeletal muscle form and function*, Windsor, On., Human Kinetics, 1996.

Moore M., Measurement of joint motion: part 2 technique of goniometry. *Phys. Ther. rev.* 29:256-264, 1949.

Moussavi Z., Cooper J., and Shwedyk E., Fatigue pattern of trapezius in relation to its functional role, *Proceedings of 18th IEEE EMB Conference*, pp. 107, Nov. 1996.

Newell D. and Nichols P., Accuracy of estimating neck movements. *Ann Phys. Med.*, 8:120-124, 1965.

Norkin C. C., and Levangie P. K., *Joint structure and function*, 2nd Ed., Philadelphia: FA., Davis, 1992.

Oberg T., Sandsjo L., Kadefors R. and Larsson S. E., Electromyographic changes in work-related myalgia of the trapezius muscle. *Eur. J. Applied Physiology,* 65:251-257, 1992.

Palmerud G., Kadefors R., et al., "Voluntary redistribution of muscle activity in human shoulder muscles", *Ergonomics,* 38(4): 806-815, 1995.

Panjabi M. and White A., Basic biomechanics of the spine, *Neurosurgery,* 1980; 7:76-93.

Papoulis A., *Signal Analysis,* McGraw-Hill, New York, NY, 1977.

Person R. S. and Mishin L. N., Auto- and cross-correlation analysis of the electrical activity of muscles, *Med. Electron. Biol. Eng.,* 2:155-159, 1964.

Polgar J., Johnson M. A. , Weightman D. and Appleton D., Data on fiber size in thirty-six human muscles: an autopsy study, *J. Neurol. Sci.,* 19: 307-318, 1973.

Portney L. G. and Watkins M. P., *Foundation of Clinical Research,* Appleton & Lange, Norwalk, Connecticut, 1993.

Safaee-Rad R., Shwedyk E. and Quanbury A.O., Three dimensional measurement system for functional arm motion. *Med. & Biol. Eng. & Comp.,* 28:569-574, 1990.

Shwedyk E., Balasubramanian R. and Scott R.N., A nonstationary model for electromyogram. *IEEE Trans. On Biomed. Eng.,* 24(5):417-424, 1977.

Simons D. G., *Myofascial Pain Syndrome Due to Trigger Points,* Gebauer Company, Cleveland, Ohio, 1987.

Simons D. G., *New Trends in Referred Pain and Hyperalgesia*, Elsevier Science Publishers, Chapter 28, 1993.

Soo K C., Guiloff R. J., Oh A., et al., Innervation of the trapezius muscle: a study in patients undergoing neck dissections, *Head & Neck*, 12: 488-495, 1990

Stacey R. J., O'Leary S. T. and Hamlyn P. J., The innervation of the trapezius muscle: a cervical motor supply, *J. Craniomaxillofac. Surg.*, 23(4): 250-251, 1995.

Storms H., System of joint measurement. *Phys Ther Rev.*, 35:369-371, 1955.

Stulen F.B. and De Luca C.J., Frequency parameters of the myoelectric signal as a measure of muscle conduction velocity. *IEEE Trans. on Biomedical engineering*, 28(7):515-519, July 1981.

Sundelin G. and Hagberg M., Electromyographic signs of shoulder muscle fatigue in repetitive arm work paced by the methods-time measurement system. *Scand. J. Work Environ. Health*, 18:262-268, 1992.

Travell J., and Simons D., *Myofascial Pain and Dysfunction: the trigger point manual.* Baltimore, Md., Williams & Wilkins, 1983.

Tucci S., Hicks J., Cross E., Campbell W. and Danoff J., Cervical motion assessment: A new, simple and accurate method. *Arch. Phys. Med. Rehabil.*, 67:225-230, 1986.

Uhlig Y., Weber B. R., Grob D. and Muntener M., Fiber composition and fiber transformations in neck muscles of patients with dysfunction of the cervical spine, *J. Orthop. Res.* 13(2): 240-249, 1995.

Whittle M. W., Calibration and performance of a three-dimensional television system for kinematic analysis. *J. Biomechanics*, 15(3):185-96, 1982.